UNIVERSITY OF SOUTHERN CALIFORNIA
DEPARTMENT OF CIVIL ENGINEERING

ATTENUATION OF SEISMIC INTENSITY IN THE BALKAN COUNTRIES

by

M. D. Trifunac, V. W. Lee, H. Cao and M. I. Todorovska

Report No. 88-01

April, 1988

ABSTRACT

The parameters of the Gaussian distribution functions (average and standard deviation) of hypocentral distances to selected isoseisms, are presented for Albania, Greece, Bulgaria, Romania, Turkey and Yugoslavia. The results apply for the Medvedev-Karnik-Sponheuer (MKS) intensity, provided that all data is corrected to a unified MKS equivalent intensity as defined by Shebalin et al. (1974). The results should be of general value in macroseismic studies in the Balkan countries, but are essential for the development of microzonation maps when the seismicity is described in terms of the locally available intensity catalogues.

Except for the Vrancea region in Romania and south-west Turkey, the observed attenuation of the intensities versus the hypocentral distance is similar to the attenuation of the Modified Mercalli Intensity (MMI) in the western United States of America. This finding should facilitate the use of other empirical scaling relations, developed in California, for various predictions of the characteristics of strong earthquake shaking in the Balkan countries.

INTRODUCTION

For the probabilistic description of strong earthquake ground motion it is necessary to have data on the expected values and on the standard deviation of the intensity of shaking at a point for a given maximum earthquake intensity and for a given epicentral distance. Such results are essential for computation of the seismic risk in the region only with short or without any instrumental seismicity records. The subject of the intensity attenuation with distance has been studied extensively, but most investigators have focused only on the description of the mean trends and little or no attention has been paid to the scatter of observed data, although it is recognized that this scatter is very important (e.g. Gupta and Nuttli, 1976; Howell and Schultz, 1975; Bollinger, 1977). With the development of the Uniform Risk Spectrum technique (Anderson and Trifunac, 1977; Lee and Trifunac, 1985) and its application in the new microzonation method (Lee, 1987; Trifunac, 1988) the need for the probabilistic description of the attenuation of intensity with distance grew and the results of several studies, in different geologic and tectonic settings are now available (Anderson, 1978; Gupta and Trifunac, 1988). A description of the attenuation of intensities with single curve through the mean trend neglects the scatter in the data and is therefore incomplete.

The Uniform Risk Spectrum (URS) method offers a systematic procedure, which incorporates in a balanced way, (1) the seismicity of various sources in the area surrounding the site, (2) the geometrical distribution and the shape of earthquake sources, (3) attenuation along different geological paths, and (4) the local soil and geologic conditions, for determination of the distribution functions of the levels of strong ground shaking. This method has been developed first for the computation of the site specific design spectra of important structures (Trifunac et al., 1979; 1987c; 1987d), but it can be used also for detailed mapping of seismic risk (Lee and Trifunac, 1987; Lee, 1987; Trifunac, 1988). To use this microzonation method it is necessary first to define the seismicity in the area using the

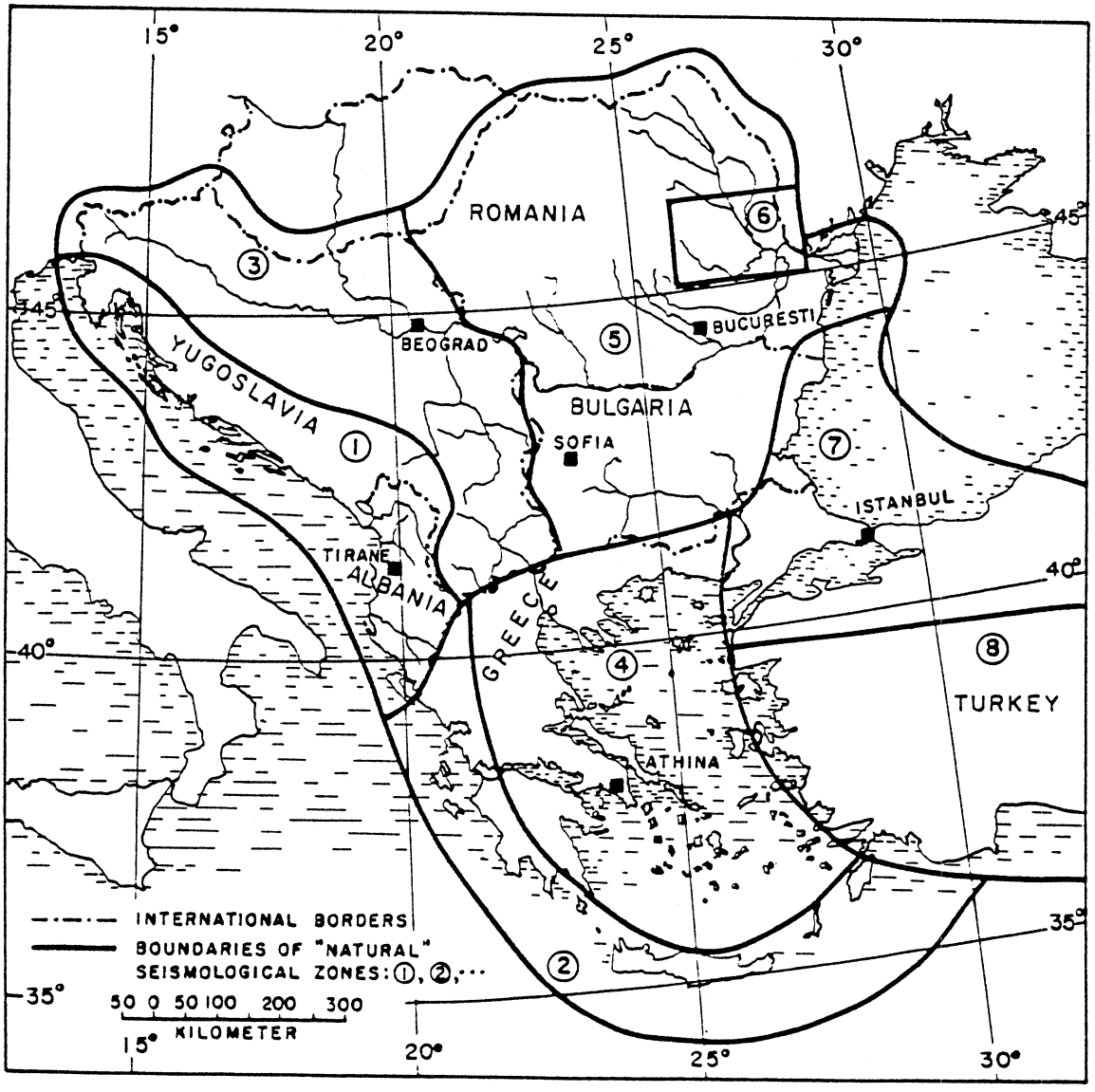

Figure 1 Boundaries of the "natural" seismological zones (1 through 8) for Balkan countries (after Shebalin et al. 1974).

data on historic seismicity (usually available only in terms of catalogues containing non-instrumental data, and in terms of the seismic intensity scales). Even when such data is readily available, it is seldom in the form that it can be used directly, because the computer programs for computation of the Uniform Risk Spectra, URS, (Lee and Trifunac, 1985) requires $P\{I < I_1|I_0, \Delta\}$ that is the probability that the intensity I will take values less than I_1 at a site at distance Δ from the source and when the epicentral intensity is I_0. The hypocentral distance $\Delta = (R^2 + H^2)^{1/2}$, where R is the epicentral distance and H is the depth of focus, and I_1 is some selected intensity such that $I_1 \leq I_0$. Anderson (1978) has shown how $P\{I < I_1|I_0, \Delta\}$ can be developed from the maps of contoured isoseismals in the United States and Gupta and Trifunac (1988) have applied this method to the Indian subcontinent. The purpose of this work is to present similar analyses for the Balkan countries in south-eastern Europe, and thus to enable the use of the URS method for selection of site specific design spectra and for the development of micro and macrozonation maps there.

To carry out the seismic risk calculations it is also necessary to have the relationships between the local intensity scales and the actually recorded amplitudes and duration of strong earthquake ground motion (e.g. Trifunac and Lee, 1987a,b). At present there is enough recorded data in the western United States and in Japan to develop such empirical correlations. In other parts of the world, including the Balkan region (Figure 1) the data available at this time is not adequate to determine such correlations independently. Though such analyses are beyond the scope of this work, it is important to note this here, because the development of $P\{I < I_1|I_0, \Delta\}$ functions is necessary for the implementation of seismic risk and microzonation calculations, but not sufficient, unless it is carried out together with the development of the direct empirical scaling of intensities with the data actually recorded in the area. With the recent completion of the strong motion data base for Yugoslavia (Jordanovski et al., 1987) it will become possible to initiate the work on this task in the near future.

DESCRIPTION OF DATA

The data used in this work (Figure 2) comes from the "Catalogue of Earthquakes" edited by Shebalin, Kárnik and Hadžievski (1974). This report presents data on isoseismals for the entire Balkan region and the western part of Turkey with $I_0 \geq$ VIII for the years prior to 1800, $I_0 \geq$ VII for the period 1801 to 1900 and $I_0 >$ VI for the period 1901 to 1970. For the period 1901 to 1970, 454 isoseismal maps have been presented and chosen for publication. Of these 304 were sufficiently complete for the requirements of this analysis.

Various seismic intensity scales have been in use in the Balkan region during different periods, and different interpretations of similar scales in the neighboring countries are portrayed by the maps which are presented in this "Catalogue of Earthquakes." Their final relationship is presented in Figure 3. Some of these scales were used differently during different periods. For example, the scales used by Prof. Mihailović changed with time and have been labeled therefore as: RF-M (used before 1912-1914), FM-M (used between 1912-1913 and 1922-1923) and MCS-M (used from 1922 and 1923 to 1945-1950). The detailed review of the mutual relationships of different scales and the empirical relationships for their conversion to the standard MKS scale have been presented by Shebalin (1969). Since one of the aims of Shebalin et al. (1974) has been to "homogenize" and to "unify" the method of presentation of isoseismal maps for the whole Balkan region, a set of "generalized" isoseismals which neglect the "local effects on the earth surface have been drawn." These generalized and smoothed isoseismals were chosen by us as the data base for this project.

In their analysis on the attenuation of intensities with epicentral distance Shebalin et al. (1974) considered both "technical" and "natural" boundaries between different geographical zones. The "technical" boundaries were considered because of the possible

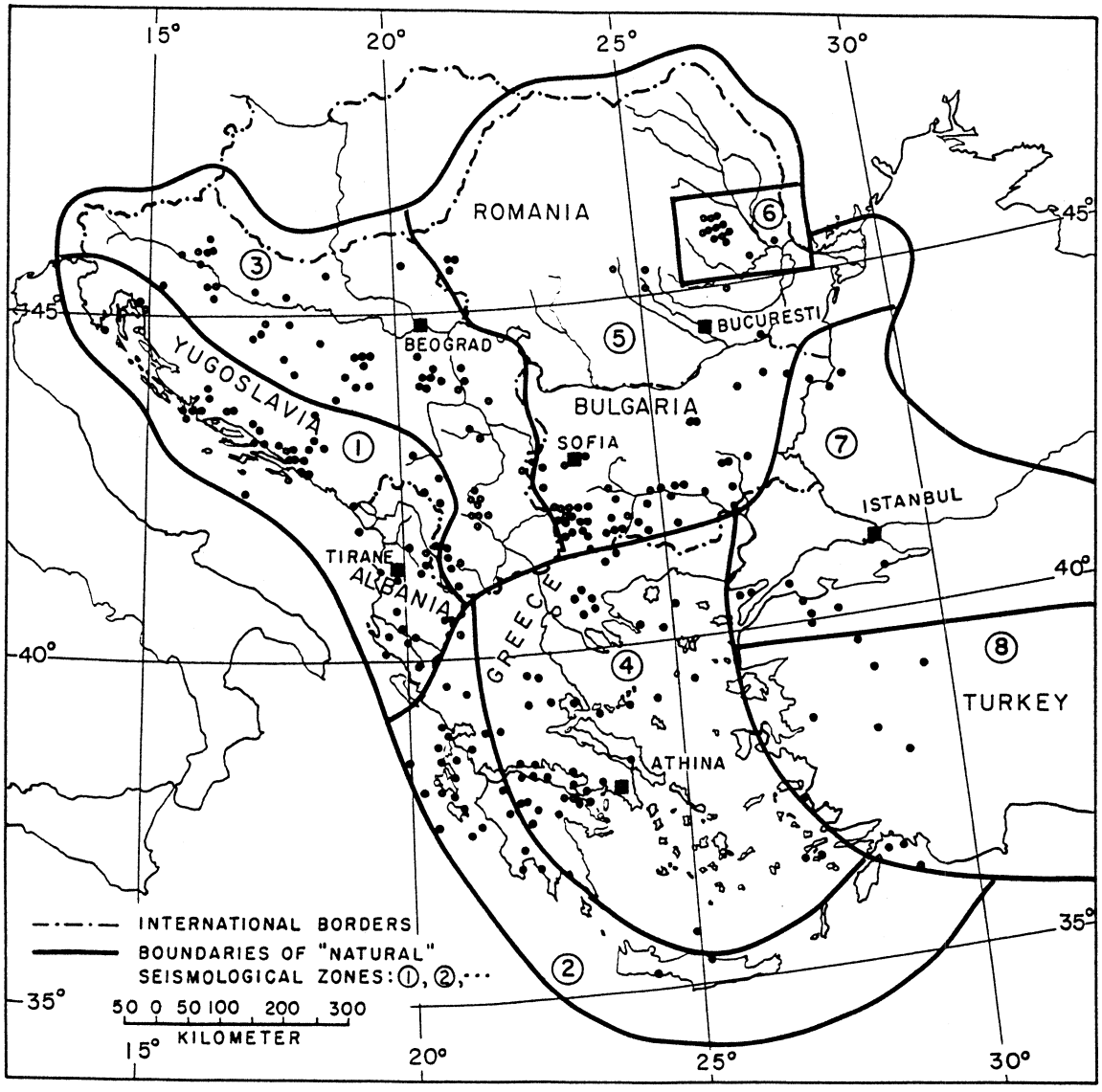

Figure 2 Epicenters of 304 earthquakes selected for this study.

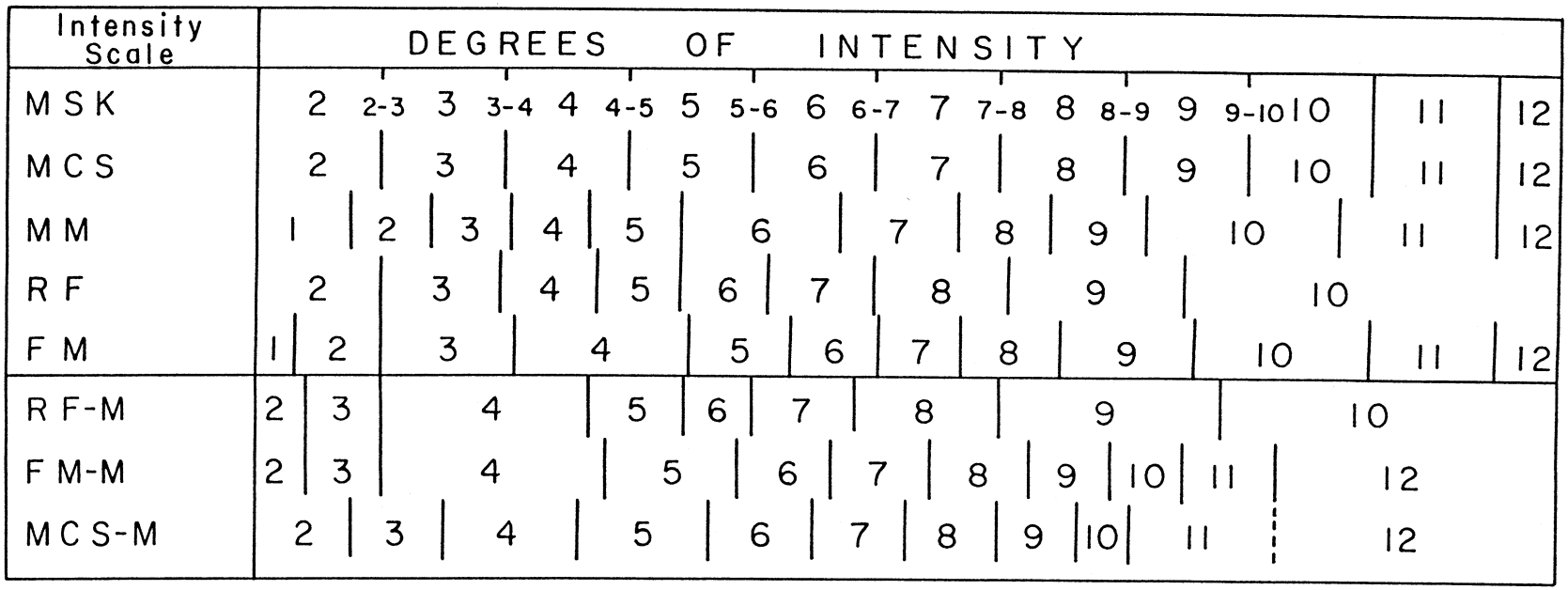

Figure 3 Correlation of seismic intensity scales used in the Balkan region (after Shebalin, 1969).

differences in national practices in the determination of the relevant earthquake parameters. The "natural" seismological zones were chosen on the basis of different tectonic environment and to study the effects of this geologic environment on attenuation. In this work we have adopted the same "natural" zones as proposed by Shebalin et al. (1974). These "natural" seismological zones are (Figure 1):

1. Outer area of the Dinarides and the Illyrides,
2. From Hellenides to Crete and Rodos,
3. Inner part of the Balkan Peninsula west of Romania and Bulgaria and north of Greece,
4. Central and eastern Greece and the Aegean Sea,
5. Inner part of the Balkan Peninsula covering most of Romania and Bulgaria,
6. Vrancea zone in Romania,
7. Eastern part of Bulgaria, Marmara Sea and north-western Anatolia,
8. South-west Turkey.

Figure 2 shows the epicenters of the 304 earthquakes which were analyzed in this report.

The total number of isoseismal maps presented for the Balkan project by Shebalin et al. (1974) does not represent the number and the actual distribution of the earthquakes in this area. This results from the non-uniform characteristics and the various levels of completeness of different national catalogues. For instance, many maps with $I_0 = \mathrm{V}$ have been included for the territory of Macedonia, while for Turkey maps were missing even for

some earthquakes with I_0 = IX. There were many variations in the style of presentation in the original national catalogues and little or no use of the data from neighboring territories.

The isoseismals have been drawn either to envelope all points with given intensity, to outline the zones with a larger number of the same reported intensity allowing for small groups of different intensities to be represented by "intensity islands," or they were drawn according to some smoothing principle. While these different methods may offer certain advantages in their respective countries, it was necessary for the investigators of the Balkan Project to choose some unified method of presentation and to show the "complete macroseismic information in a homogeneous form." This impressive work on revision, completion, generalization and final drawing of isoseismal maps has been carried out by N. V. Shebalin and I. Todorov (Shebalin et al., 1974). It is only thanks to this effort that our present analysis is possible.

METHODS OF ANALYSIS

Figure 4 (redrawn from Anderson, 1978) shows sixteen radii drawn from the epicenter. The distances to each isoseismal in the direction of these radii (e.g. R_6) were measured, tabulated and stored into computer files. When an isoseism was drawn over water or with a broken line it was not included in the data base (e.g. R_5 on line 16). After reading all the maps in this manner the data was grouped according to the maximum intensity, I_0, and from that point on the analysis followed the same steps as described in Anderson (1978).

Figures 5a through 5h present the distribution of the available data with respect to the focal depth and the hypocentral distances $\Delta_i = (R_i^2 + H^2)^{1/2}$, where R_i represent the radii (or epicentral distances) for a given isoseism and H is the focal depth of the corresponding earthquakes. Bottom portions of Figures 5 show histograms of the number

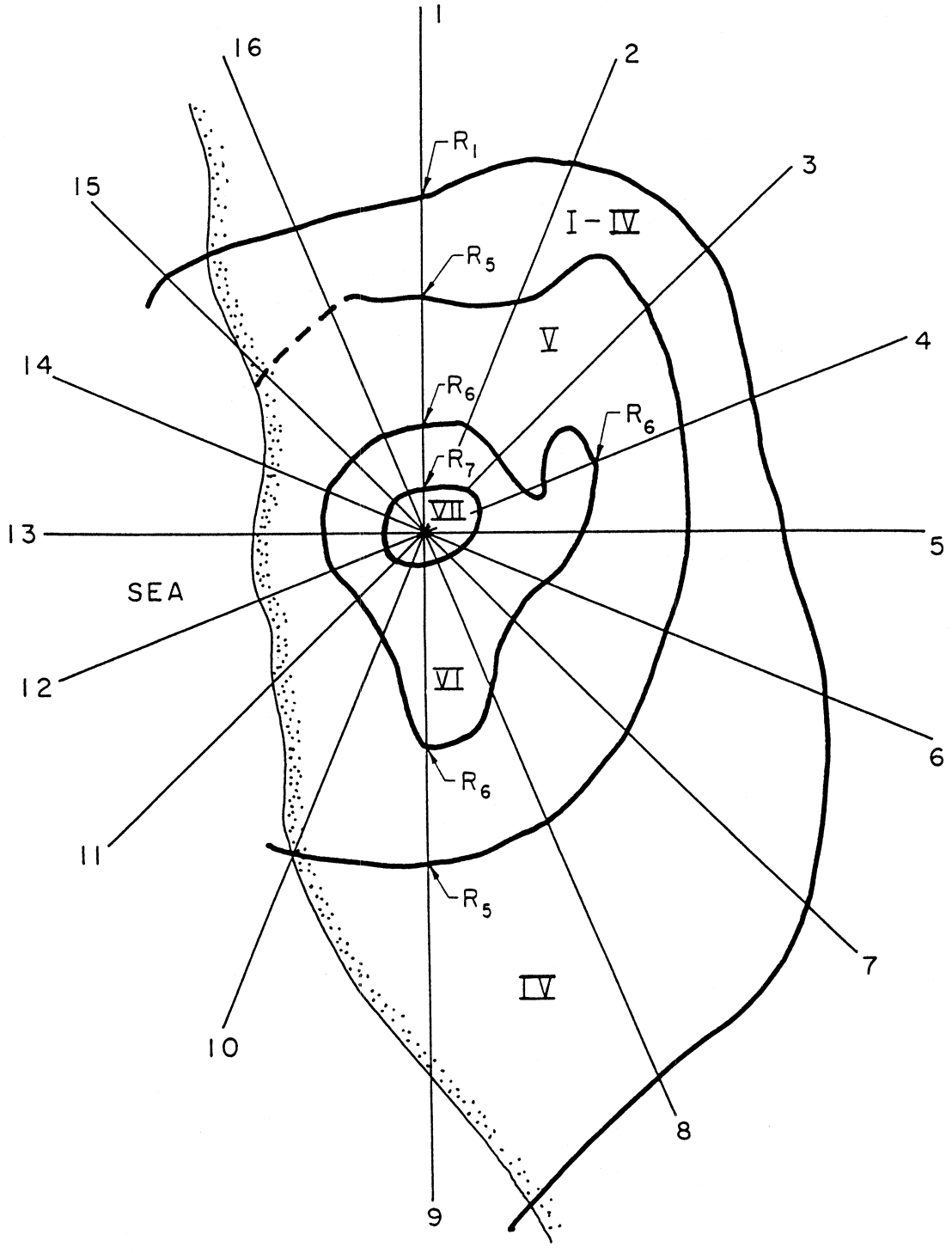

Figure 4 Example of isoseismal map showing the convention used to measure 16 radii to I_1.

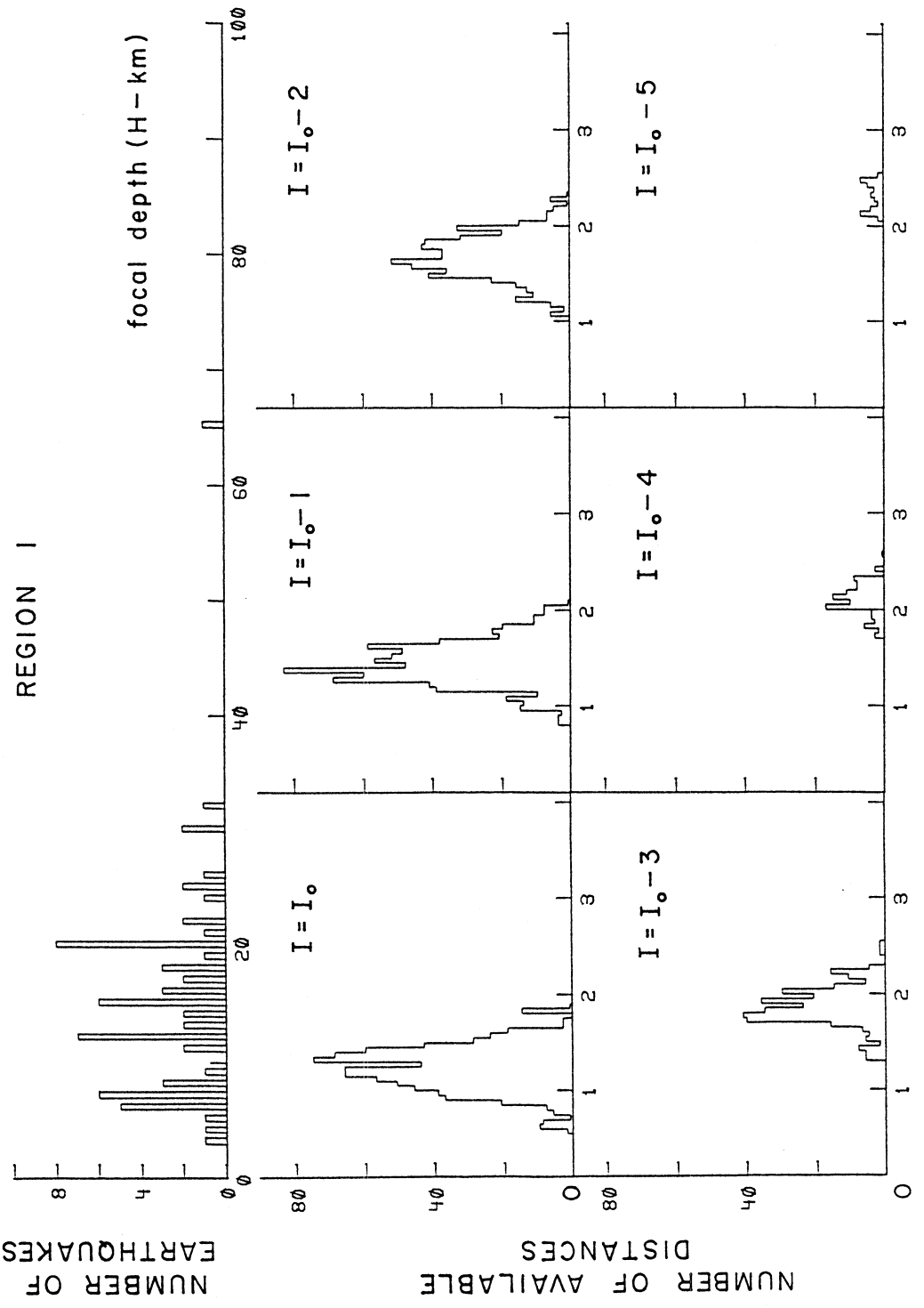

Figure 5a Top: Histogram of focal depths, for region 1. Bottom: Histograms of $\log_{10}(\Delta)$ for isoseismals of intensity $I = I_0, I_0 - 1, \ldots I_0 - 5$, for region 1.

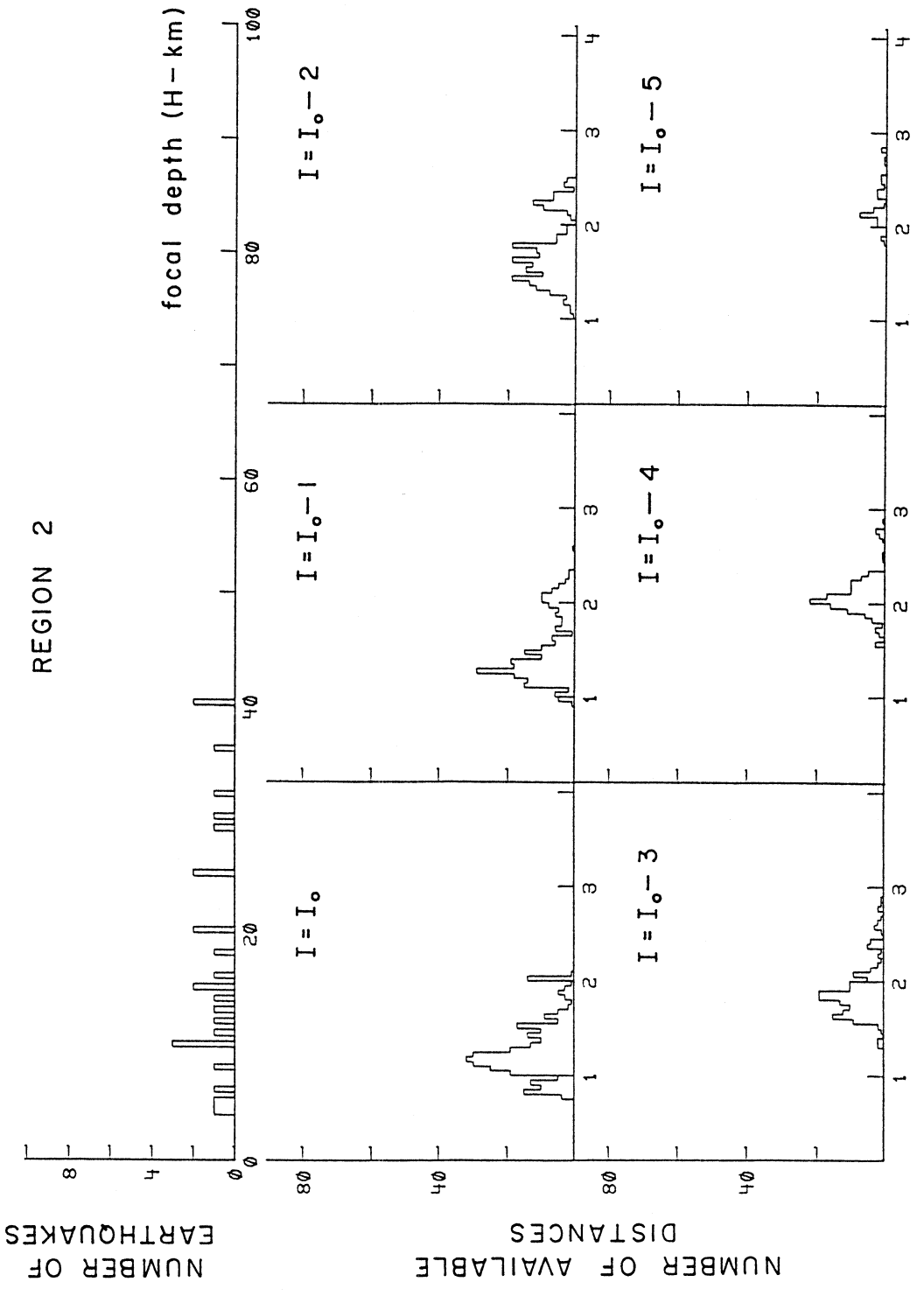

Figure 5b Top: Histogram of focal depths, for region 2. Bottom: Histograms of $\log_{10}(\Delta)$ for isoseismals of intensity $I = I_0, I_0 - 1, \ldots I_0 - 5$, for region 2.

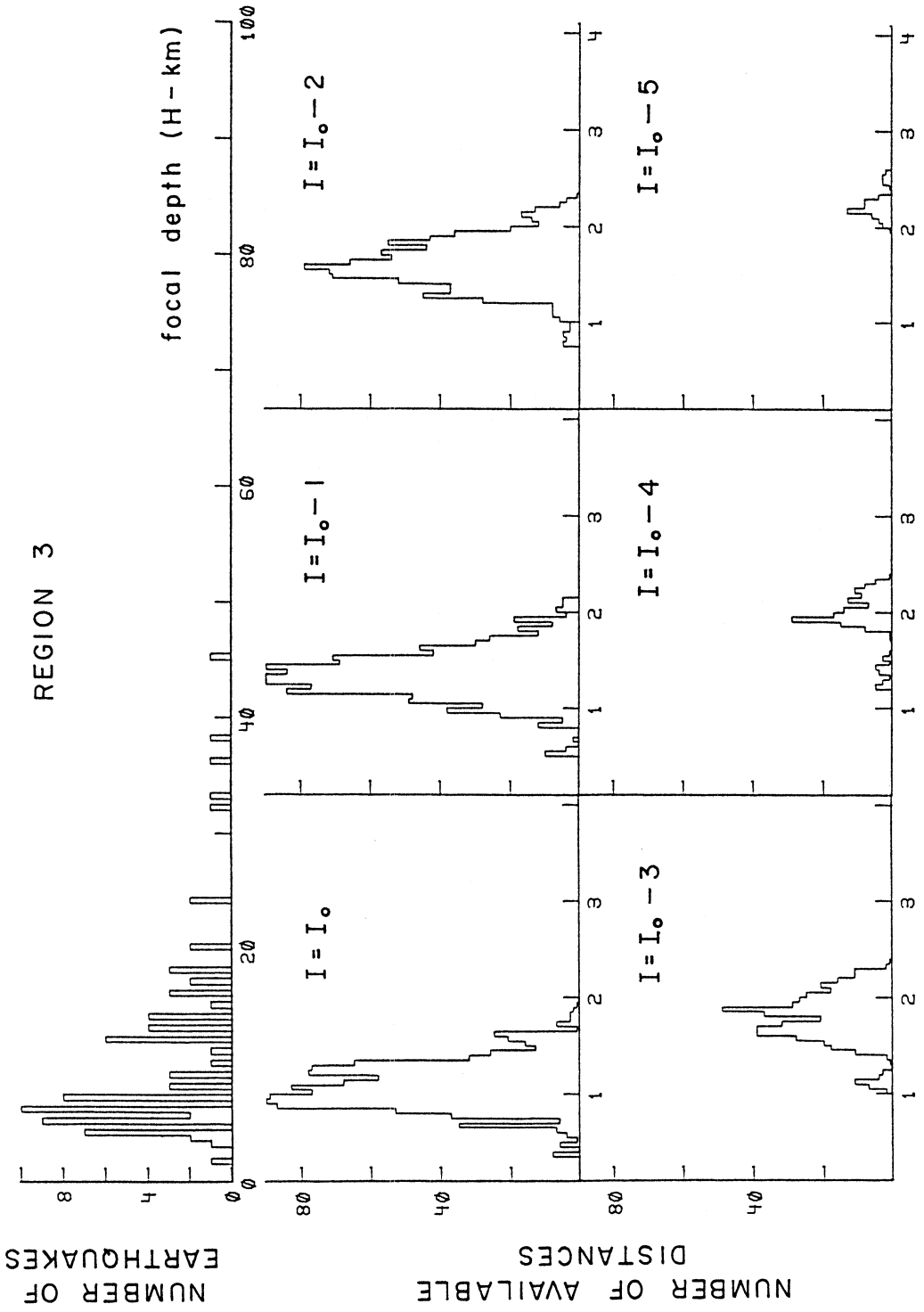

Figure 5c Top: Histogram of focal depths, for region 3. Bottom: Histograms of $\log_{10}(\Delta)$ for isoseismals of intensity $I = I_0, I_0 - 1, \ldots I_0 - 5$, for region 3.

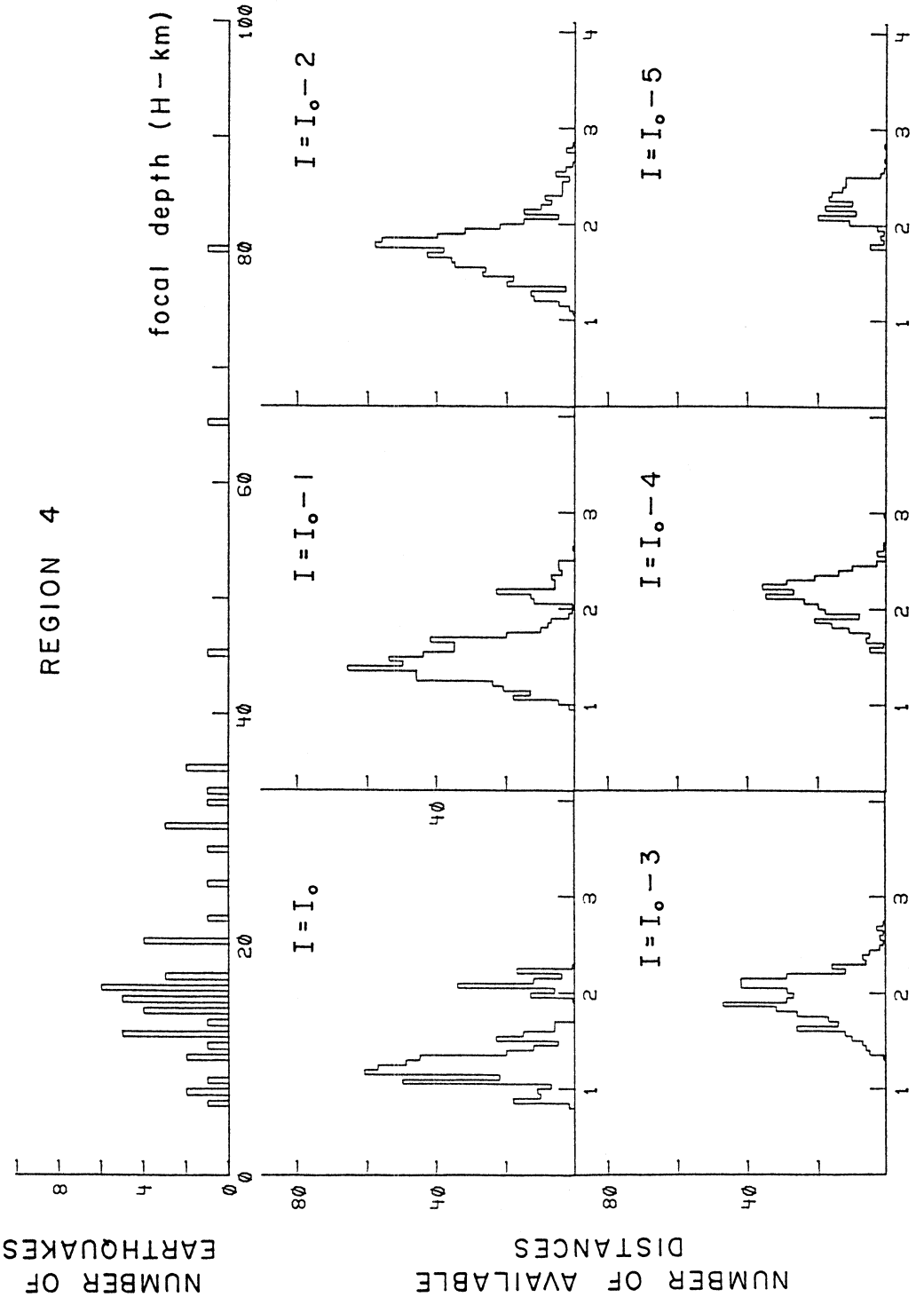

Figure 5d Top: Histogram of focal depths, for region 4. Bottom: Histograms of $\log_{10}(\Delta)$ for isoseismals of intensity $I = I_0, I_0 - 1, \ldots I_0 - 5$, for region 4.

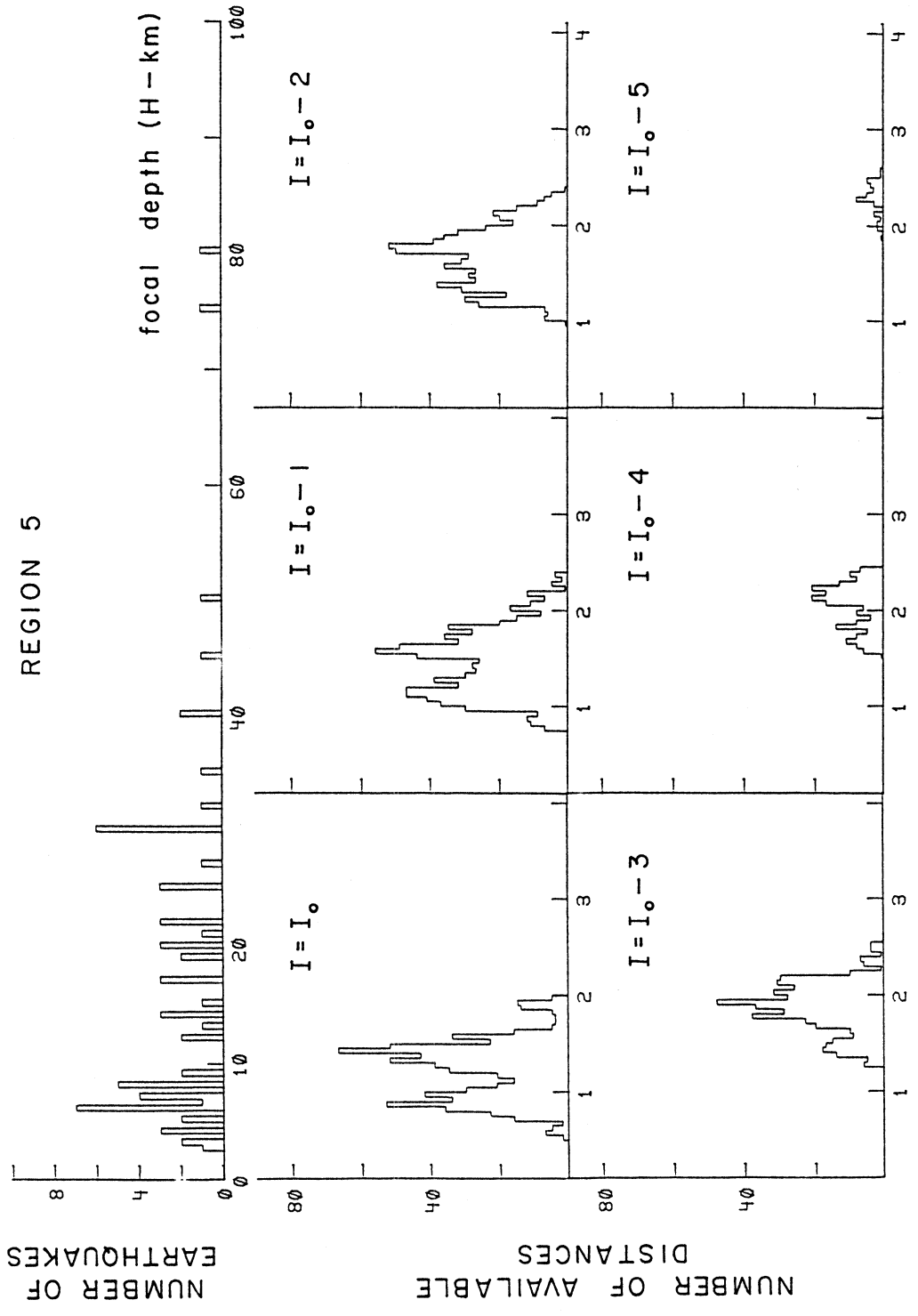

Figure 5e Top: Histogram of focal depths, for region 5. Bottom: Histograms of $\log_{10}(\Delta)$ for isoseismals of intensity $I = I_0, I_0 - 1, \ldots I_0 - 5$, for region 5.

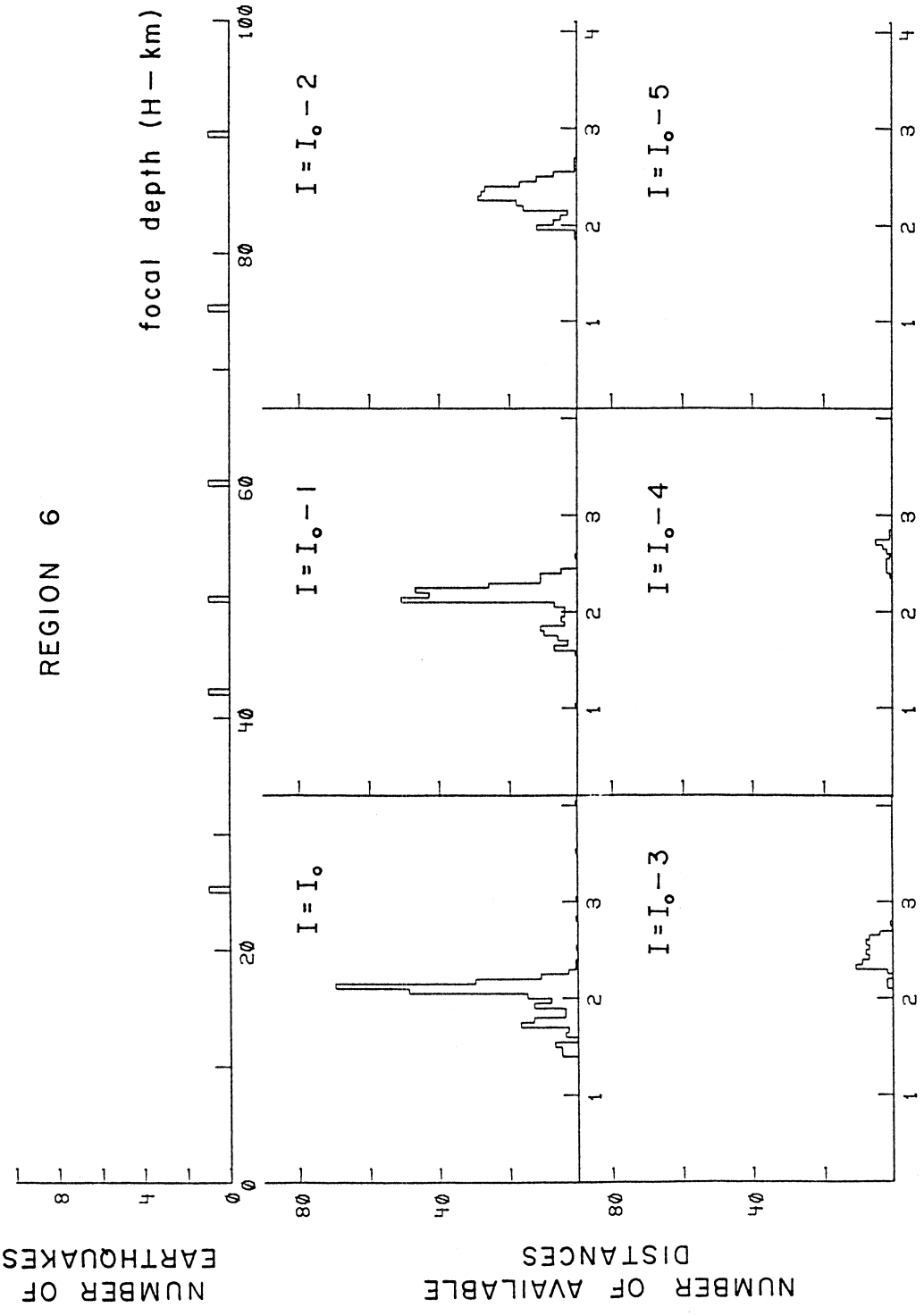

Figure 5f Top: Histogram of focal depths, for region 6. Bottom: Histograms of $\log_{10}(\Delta)$ for isoseismals of intensity $I = I_0, I_0 - 1, \ldots I_0 - 5$, for region 6.

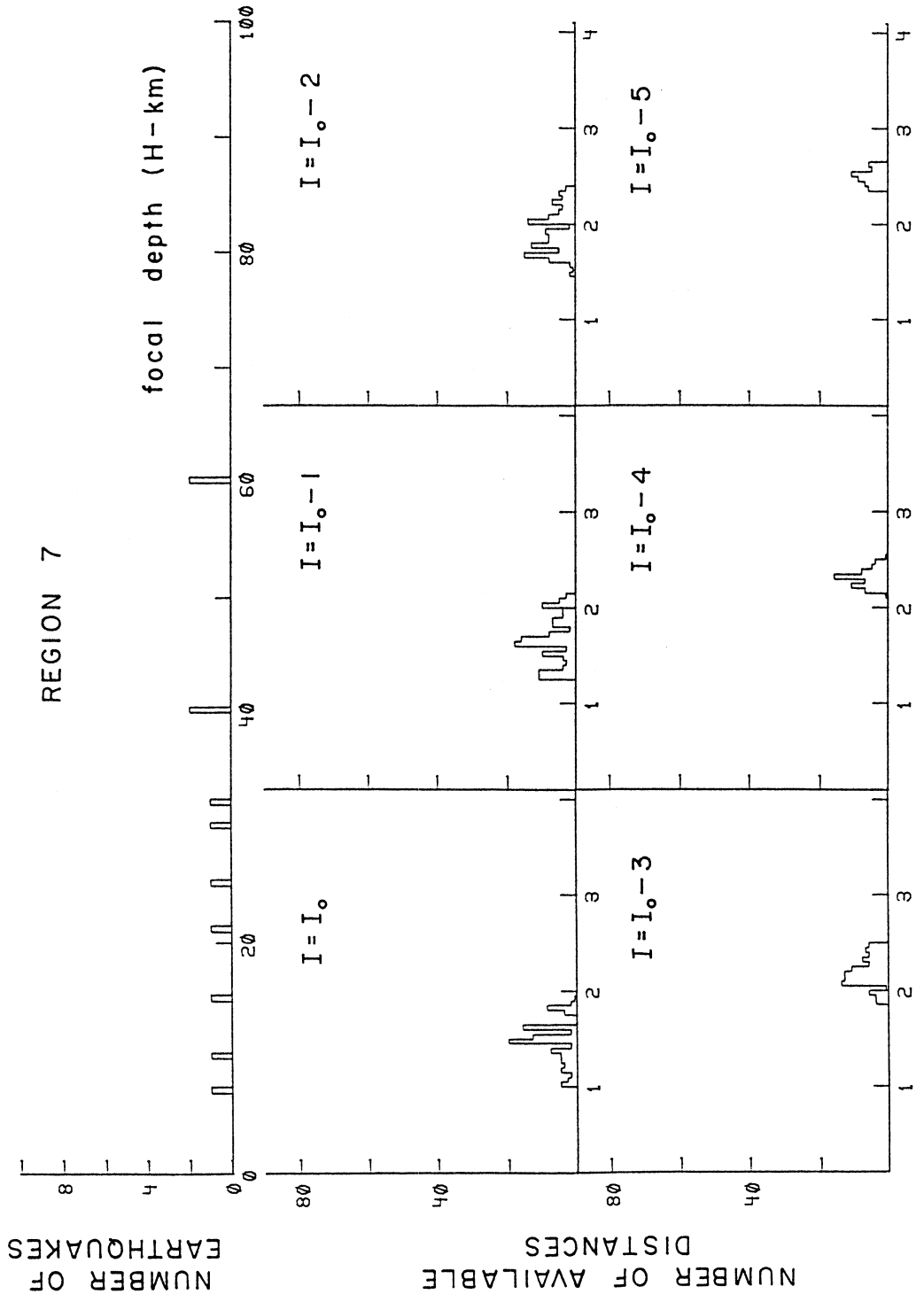

Figure 5g Top: Histogram of focal depths, for region 7. Bottom: Histograms of $\log_{10}(\Delta)$ for isoseismals of intensity $I = I_0, I_0 - 1, \ldots I_0 - 5$, for region 7.

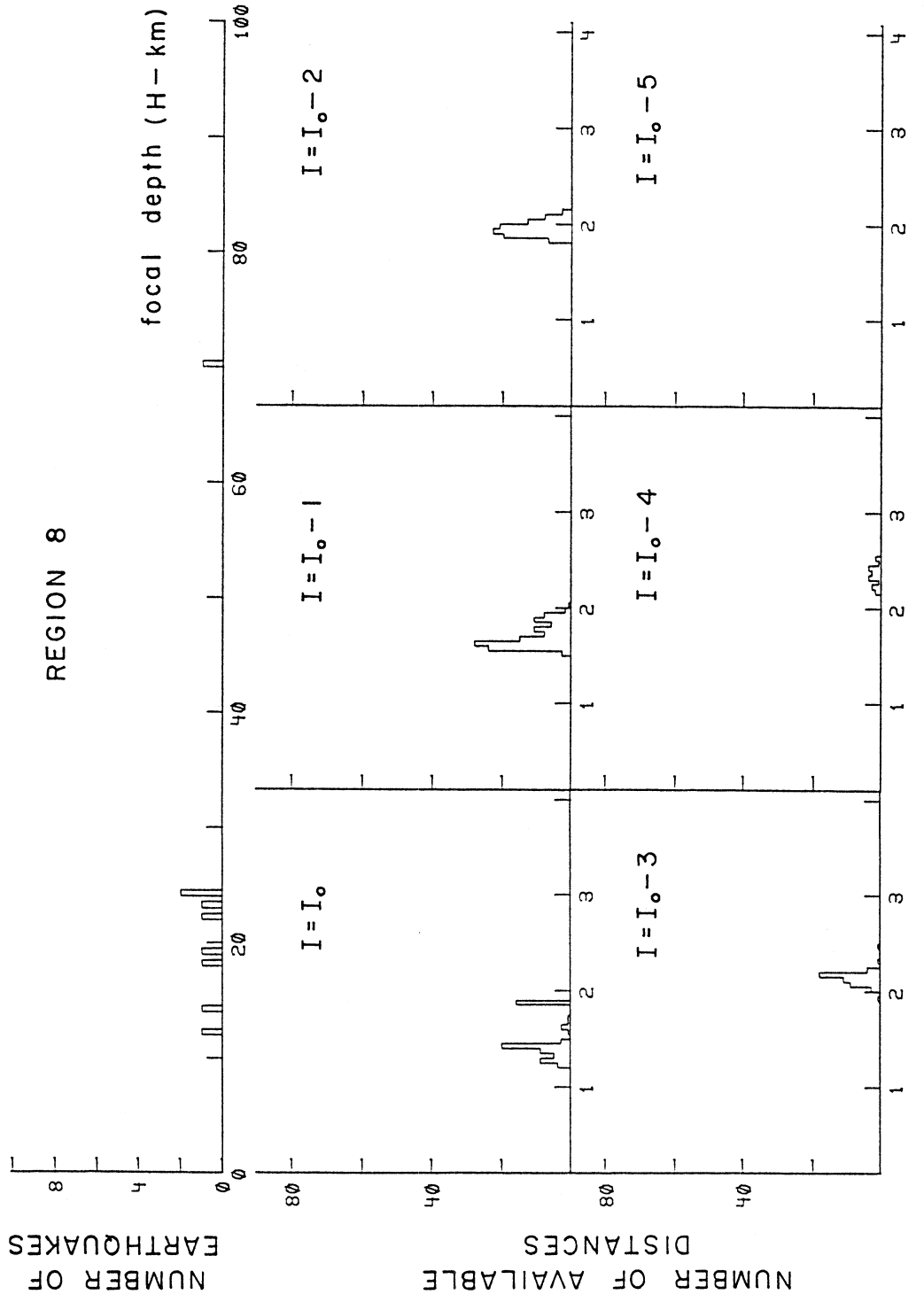

Figure 5h Top: Histogram of focal depths, for region 8. Bottom: Histograms of $\log_{10}(\Delta)$ for isoseismals of intensity $I = I_0, I_0 - 1, \ldots I_0 - 5$, for region 8.

of the available distances, Δ_i, for intensities $I = I_0$, $I = I_0 - 1, \ldots$ and $I = I_0 - 5$, plotted versus $\log_{10}\Delta$. It is seen that the number of the available data, for regions 2, 6, 7 and 8 is small (Tables 1.1 through 1.8). Therefore, the results of this analysis as presented here for these regions must be taken only as preliminary until more complete data base becomes available. For completeness of this presentation and to facilitate comparison with the results for regions 1, 3, 4 and 5 we have included here all preliminary results for the regions 2, 6, 7 and 8.

All the measured distances, Δ_i, for the I_1 isoseismals corresponding to earthquakes with epicentral intensity I_0, $(I_1 \leq I_0)$, were grouped in increasing order forming the ordered set $\Delta_1 \leq \Delta_2 \leq \ldots \leq \Delta_i \leq \ldots \leq \Delta_{N_{I_0,I_1}}$. Here N_{I_0,I_1}, is the number of the available distances for the isoseismal I_1 corresponding to earthquakes with epicentral intensity I_0. The probability

$$P\{I < I_1 | I_0, \Delta\} = P_{I_0,I_1}(\Delta)$$

where $P_{I_0,I_1}(\Delta)$ is the cummulative distribution function for the hypocentral distances to the I_1 isoseismal when the epicentral intensity is I_0. $P_{I_0,I_1}(\Delta)$ can be approximated by the following expression

$$P_{I_0,I_1}(\Delta) = \frac{i}{N_{I_0,I_1}} \quad , \quad \Delta_i \leq \Delta < \Delta_{i+1} \; . \tag{1}$$

The Gaussian curve $\hat{P}_{I_0,I_1}(\Delta)$ to approximate the distribution (1) is of the form

$$\hat{P}_{I_0,I_1}(\Delta) = \frac{1}{\sigma_{I_0,I_1}} \sqrt{\frac{1}{2\pi}} \int_{-\infty}^{\log_{10}\Delta} \exp\left[-\frac{1}{2}\left(\frac{\mu_{I_0,I_1} - x}{\sigma_{I_0,I_1}}\right)^2\right] dx \tag{2}$$

where μ_{I_0,I_1} and σ_{I_0,I_1} are the mean and the standard deviation of the data in the ordered set, that can be found by a least square procedure. Finally, the maximum difference between the observed distribution function and the Gaussian approximation of the same function, ϵ_{I_0,I_1}, can be found as

$$\epsilon_{I_0,I_1} = \max_i \{|\hat{P}_{I_0,I_1}(\Delta_i) - P_{I_0,I_1}(\Delta_i)|\} \quad .$$

Table 1.1 Average and standard deviation of the logarithm of the hypocentral distance in kilometers to isoseism enclosing the area with $I \geq I_1$.

REGION 1

EPICENTRAL INTENSITY, I_o		INTENSITY I_1							
		3	4	5	6	7	8	9	10
3.0									
3.5									
4.0									
4.5									
5.0	7		5 38 1.805 .130	7 90 1.572 .118					
5.5	1		1 6 1.696 .051	1 9 1.457 .039					
6.0	17	10 59 2.010 .156	13 119 1.787 .231	17 201 1.517 .173	14 189 1.231 .192				
6.5	5	1 8 2.220 .029	5 29 1.889 .092	5 51 1.645 .218	5 80 1.320 .180				
7.0	12	2 6 2.104 .064	8 85 1.803 .196	10 119 1.640 .172	11 135 1.380 .196	11 135 1.172 .184			
7.5	3	2 10 2.149 .154	1 3 2.155 .047	3 29 1.768 .190	3 45 1.492 .193	3 48 1.243 .161			
8.0	8	3 10 2.282 .188	5 43 2.138 .114	8 81 1.852 .132	8 92 1.597 .212	8 114 1.357 .157	6 91 1.117 .107		
8.5	2				2 17 1.647 .159		2 32 1.138 .265		
9.0	10	1 5 2.394 .082	5 29 2.309 .131	5 39 2.041 .189	6 73 1.796 .101	7 93 1.541 .104	8 112 1.302 .083	6 87 1.171 .060	
9.5									
10.0									
	65								

Table 1.2 Average and standard deviation of the logarithm of the hypocentral distance in kilometers to isoseism enclosing the area with $I \geq I_1$.

REGION 2

EPICENTRAL INTENSITY, I_o		INTENSITY I_1							
		3	4	5	6	7	8	9	10
3.0									
3.5									
4.0									
4.5									
5.0	5		5 45 1.988 .131	4 41 1.590 .094					
5.5									
6.0									
6.5									
7.0	7		6 62 1.924 .217	6 71 1.622 .171	6 78 1.336 .126	4 56 1.072 .034			
7.5									
8.0	8		7 72 2.077 .136	5 56 1.829 .156	6 66 1.530 .204	4 44 1.300 .232	8 116 1.162 .204		
8.5									
9.0	3		1 9 2.386 .058	1 16 2.024 .207	1 16 1.730 .128	2 20 1.544 .129	2 22 1.340 .076	3 36 1.275 .099	
9.5									
10.0									
	23								

Table 1.3 Average and standard deviation of the logarithm of the hypocentral distance in kilometers to isoseism enclosing the area with $I \geq I_1$.

REGION 3

EPICENTRAL INTENSITY, I_o		INTENSITY I_1							
		3	4	5	6	7	8	9	10
3.0									
3.5									
4.0									
4.5									
5.0									
5.5									
6.0	27	9 55 1.925 .253	21 188 1.710 .169	25 318 1.379 .177	25 355 1.077 .182				
6.5	5		3 26 1.817 .228	5 71 1.418 .236	5 78 1.067 .208				
7.0	29		18 214 1.780 .220	26 362 1.531 .204	26 363 1.275 .196	25 359 .972 .167			
7.5	3	2 6 2.125 .039	2 18 1.883 .053	3 41 1.540 .076	3 44 1.285 .062	3 48 1.041 .127			
8.0	7		7 45 2.009 .150	7 73 1.794 .195	7 98 1.445 .258	7 93 1.212 .228	4 56 1.089 .224		
8.5	3	1 2 2.346 .001	2 8 2.227 .029	3 29 2.058 .105	3 46 1.873 .128	3 48 1.591 .100	3 42 1.332 .057		
9.0	3		3 34 2.268 .121	3 42 2.006 .090	3 48 1.773 .200	3 48 1.577 .188	3 44 1.327 .104	2 23 1.121 .018	
9.5									
10.0	1		1 5 2.378 .036	1 14 2.157 .090	1 15 1.890 .048	1 16 1.677 .108	1 16 1.512 .118	1 15 1.326 .049	1 13 1.222 .010
	78								

Table 1.4 Average and standard deviation of the logarithm of the hypocentral distance in kilometers to isoseism enclosing the area with $I \geq I_1$.

REGION 4

EPICENTRAL INTENSITY, I_o		INTENSITY I_1							
		3	4	5	6	7	8	9	10
3.0									
3.5									
4.0									
4.5									
5.0									
5.5									
6.0	9	7 63 2.032 .148	8 100 1.802 .115	9 122 1.453 .129	6 80 1.127 .161				
6.5	3	2 21 2.112 .153	3 37 1.886 .088	2 25 1.667 .103	2 19 1.480 .058				
7.0	9	7 46 2.235 .093	9 88 2.074 .123	9 102 1.792 .141	7 93 1.511 .161	8 91 1.256 .118			
7.5	1	1 11 2.145 .055	1 10 2.020 .048	1 14 1.819 .048	1 14 1.666 .051	1 15 1.391 .080			
8.0	13	10 81 2.187 .128	13 159 2.047 .200	12 170 1.807 .242	13 162 1.527 .214	13 167 1.287 .154	11 126 1.114 .112		
8.5									
9.0	6	3 33 2.465 .140	4 42 2.264 .159	4 40 2.044 .207	5 45 1.724 .105	5 56 1.571 .111	5 59 1.422 .101	3 36 1.287 .056	
9.5	2	1 5 2.502 .093	1 15 2.391 .092	2 29 2.197 .085	2 28 1.851 .067	2 25 1.614 .076	1 15 1.424 .046	2 19 1.341 .020	
10.0	1		1 16 2.565 .046	1 7 2.417 .042	1 16 2.257 .052			1 16 1.644 .015	
	44								

Table 1.5 Average and standard deviation of the logarithm of the hypocentral distance in kilometers to isoseism enclosing the area with $I \geq I_1$.

REGION 5

EPICENTRAL INTENSITY, I_o		INTENSITY I_1							
		3	4	5	6	7	8	9	10
3.0									
3.5									
4.0									
4.5									
5.0	8	7 54 1.969 .139	8 92 1.754 .191	6 72 1.435 .054					
5.5									
6.0	25	19 166 1.940 .154	22 228 1.686 .189	22 279 1.388 .222	19 293 1.183 .220				
6.5	3	1 2 2.395 .018	3 26 1.956 .177	3 37 1.712 .167	3 41 1.317 .173				
7.0	9	7 76 1.843 .169	8 116 1.641 .178	9 114 1.297 .103	9 113 1.054 .118	7 102 .794 .117			
7.5	3	2 5 2.323 .146	2 23 1.800 .330	3 37 1.412 .259	3 41 1.160 .079	2 32 .963 .062			
8.0	6	2 14 2.141 .162	5 46 2.126 .201	6 74 1.899 .334	6 74 1.579 .233	5 56 1.277 .228	4 64 1.324 .327		
8.5									
9.0	1	1 1 2.598 .000	1 5 2.435 .024	1 11 2.228 .031	1 12 2.059 .034	1 12 1.767 .099	1 16 1.530 .074		
9.5	2	1 8 2.427 .038	1 13 2.292 .043	2 28 2.135 .054	2 30 1.942 .109	2 29 1.689 .086	2 29 1.572 .040	2 28 1.508 .017	
10.0	1			1 7 2.458 .095	1 10 2.332 .085	1 13 2.164 .040	1 16 1.911 .052	1 15 1.759 .032	1 16 1.630 .020
	58								

Table 1.6 Average and standard deviation of the logarithm of the hypocentral distance in kilometers to isoseism enclosing the area with $I \geq I_1$.

REGION 6

EPICENTRAL INTENSITY, I_o		INTENSITY I_1							
		3	4	5	6	7	8	9	10
3.0									
3.5									
4.0									
4.5	1	1 16 2.315 .069	1 16 2.146 .026						
5.0	5	5 55 2.243 .154	5 70 2.153 .170	5 80 1.927 .273					
5.5	1	1 10 2.309 .138	1 13 2.137 .031	1 15 2.078 .008					
6.0	5	3 27 2.490 .101	5 54 2.320 .081	5 69 2.149 .076	5 68 1.997 .132				
6.5	2	1 16 2.328 .130			2 32 1.981 .279				
7.0	1	1 6 2.650 .152	1 10 2.545 .133	1 14 2.412 .121	1 13 2.262 .090	1 13 2.122 .017			
7.5									
8.0	1				1 16 2.300 .054	1 16 2.175 .040	1 16 2.006 .013		
8.5									
9.0	1			1 11 2.644 .109	1 13 2.495 .134	1 16 2.345 .110	1 15 2.203 .054	1 15 2.120 .002	
9.5									
10.0									
	17								

Table 1.7 Average and standard deviation of the logarithm of the hypocentral distance in kilometers to isoseism enclosing the area with $I \geq I_1$.

REGION 7

I_o		3	4	5	6	7	8	9	10
3.0									
3.5									
4.0									
4.5									
5.0									
5.5									
6.0	4	3 17 2.408 .051	4 41 2.155 .144	4 50 1.816 .287	3 42 1.513 .297				
6.5									
7.0									
7.5									
8.0	2	2 8 2.502 .056	2 22 2.244 .062	2 30 2.070 .143	2 27 1.751 .186	2 23 1.418 .153	1 11 1.361 .018		
8.5									
9.0	2	2 12 2.629 .059	2 24 2.478 .069	2 25 2.346 .070	2 28 2.157 .089	2 23 1.758 .084	2 31 1.556 .081	2 32 1.369 .138	
9.5									
10.0	2		2 6 2.803 .020	2 11 2.520 .092	2 8 2.343 .057	2 13 2.174 .052	2 18 1.796 .080	2 20 1.672 .041	2 19 1.603 .025
	10								

EPICENTRAL INTENSITY, I_o

INTENSITY I_1

Table 1.8 Average and standard deviation of the logarithm of the hypocentral distance in kilometers to isoseism enclosing the area with $I \geq I_1$.

REGION 8

EPICENTRAL INTENSITY, I_o		INTENSITY I_1							
		3	4	5	6	7	8	9	10
3.0									
3.5									
4.0									
4.5									
5.0									
5.5									
6.0	1	1 4 2.138 .023	1 16 1.896 .068	1 16 1.611 .029	1 16 1.356 .056				
6.5									
7.0	3		1 1 2.481 .000	2 31 1.967 .076	3 43 1.797 .137	3 37 1.643 .214			
7.5									
8.0	3		1 6 2.222 .036	2 21 2.102 .053	2 21 1.922 .056	2 27 1.613 .043	1 16 1.303 .063		
8.5									
9.0	2			1 14 2.404 .065	2 19 2.186 .035	2 22 1.953 .049	2 26 1.678 .088	1 3 1.502 .064	
9.5									
10.0									
	9								

Then, this maximum difference is compared with $\epsilon^{KS}_{I_0,I_1}$, the Kolmogorov-Smirnov critical value for the 95 percent confidence level. If $\epsilon_{I_0,I_1} > \epsilon^{KS}_{I_0,I_1}$, it means that at the 95 percent confidence level the measured data is not a member of the assumed distribution $\hat{P}_{I_0,I_1}(\Delta)$ (Hoel, 1971). Figures 6a and 6b illustrate $P_{I_0,I_1}(\Delta)$ and $\hat{P}_{I_0,I_1}(\Delta)$ for region 1 and region 5 earthquakes with I_0 = VII and I_1 = IV, V, VI and VII. In the calculations those values of I_0 and I_1 were considered which were represented by 5 or more radii. In addition, the figures 6a and 6b show the "error" functions $D_{I_0,I_1}(\Delta)$ defined by

$$D_{I_0,I_1}(\Delta) = \max_i \{|\hat{P}_{I_0,I_1}(\Delta_i) - P_{I_0,I_1}(\Delta_i)|/\epsilon^{KS}_{I_0,I_1}\} .$$

The error functions give the normalized difference between the distribution of distances implied by the data and the Gaussian approximation of this data. Since $P_{I_0,I_1}(\Delta)$ is multiple valued for each distance $\Delta = \Delta_i$ (equation 1), the value of $P_{I_0,I_1}(\Delta_i)$ which leads to the largest value of $D_{I_0,I_1}(\Delta)$ is used to compute $D_{I_0,I_1}(\Delta)$ at these points. Because $\epsilon^{KS}_{I_0,I_1}$ is selected to normalize the difference between $P_{I_0,I_1}(\Delta)$ and $\hat{P}_{I_0,I_1}(\Delta)$, whenever $D_{I_0,I_1}(\Delta) > 1.0$ at some value of Δ, $\hat{P}_{I_0,I_1}(\Delta)$ is rejected by the Kolmogorov-Smirnov test, at the 95 percent confidence level, as an acceptable model for $P_{I_0,I_1}(\Delta)$. By examining $D_{I_0,I_1}(\Delta)$, then, it is possible to tell how well the model $\hat{P}_{I_0,I_1}(\Delta)$ approximates $P_{I_0,I_1}(\Delta)$. For example, in Figure 6b the "error" function $D_{I_0,I_1}(\Delta)$ is larger then 1 for $I_1 = I_0, I_0$ = VII, and I_1 = V, for distances Δ around 5, 7 to 8 and 25 km respectively. In Figure 6a, $D_{I_0,I_1}(\Delta) < 1$ for all R. In this work, however, we will accept the approximate Gaussian distribution model given by equation (2), even when some $D_{I_0,I_1}(\Delta)$ functions exceed 1 locally, because the overall amplitudes of $D_{I_0,I_1}(\Delta)$ are much less than 1, because many of the peaks of $D_{I_0,I_1}(\Delta)$ which exceed 1 at 95 percent confidence would become acceptable at 90 percent confidence level, and because many discrepancies between the data and the model result from incomplete data rather than from some obvious physical reason for rejecting the Gaussian nature of the assumed distribution. Detailed plots for all 8 regions and for all intensities, for which there were sufficient data, have been analyzed and plotted

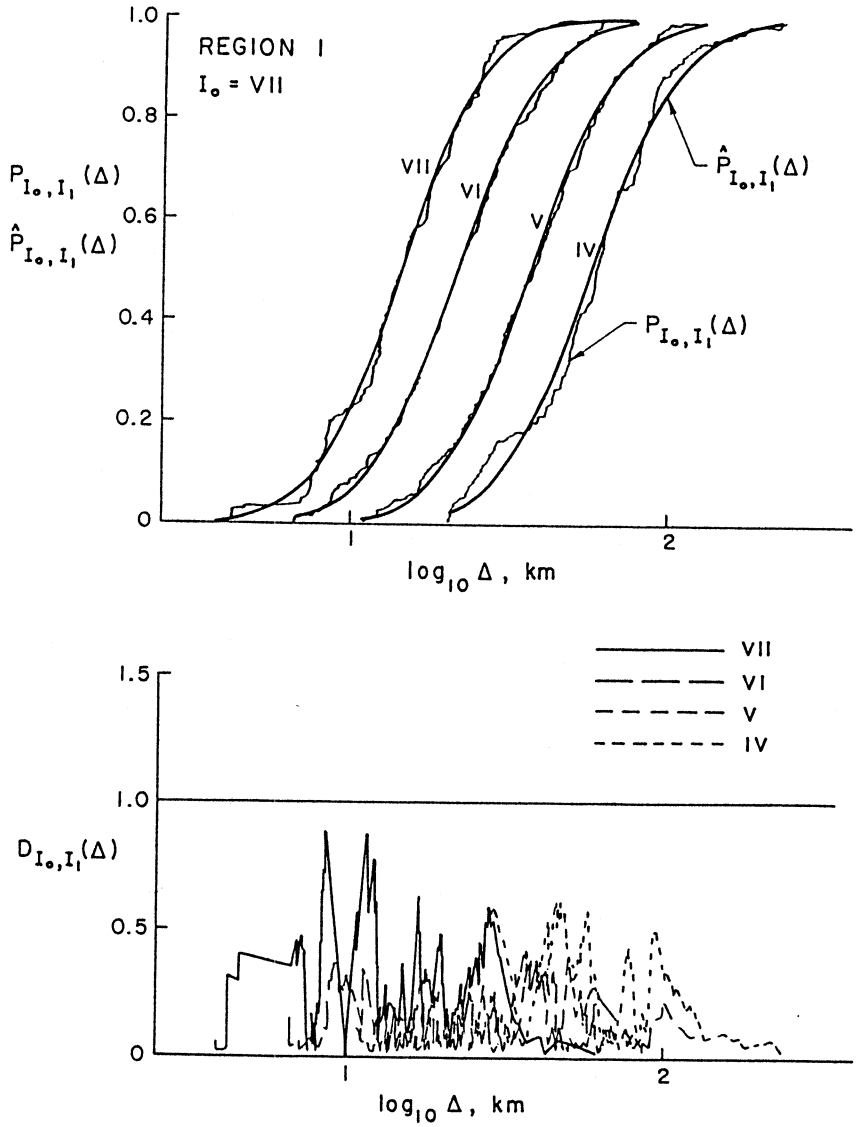

Figure 6a Top: Empirical distribution functions versus $\log_{10}(\Delta)$ for region 1. The staircase function represents $P_{I_0,I_1}(\Delta)$ determined directly from the data for I_0 = VII and I_1 = VII, VI, V and IV. The smooth curve is the corresponding Gaussian distribution $\hat{P}_{I_0,I_1}(\Delta)$, defined in equation (2). Bottom: The error function $D_{I_0,I_1}(\Delta)$, that shows the difference between the Gaussian and the empirical distributions, normalized to the Kolmogorov-Smirnov critical (95 percent confidence) value for the number of data in this set.

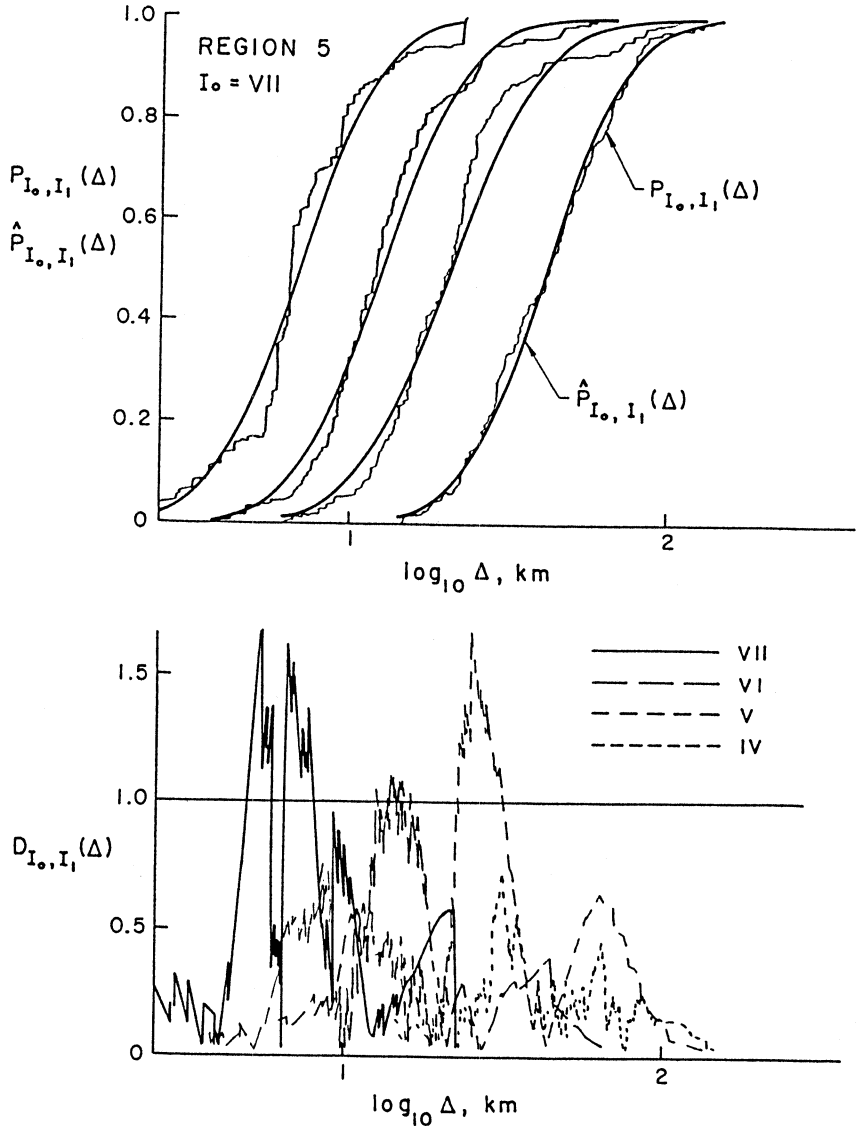

Figure 6b Top: Empirical distribution functions versus $\log_{10}(\Delta)$ for region 5. The staircase function represents $P_{I_0,I_1}(\Delta)$ determined directly from the data for I_0 = VII and I_1 = VII, VI, V and IV. The smooth curve is the corresponding Gaussian distribution $\hat{P}_{I_0,I_1}(\Delta)$, defined in equation (2). Bottom: The error function $D_{I_0,I_1}(\Delta)$, that shows the difference between the Gaussian and the empirical distributions, normalized to the Kolmogorov-Smirnov critical (95 percent confidence) value for the number of data in this set.

in the manner illustrated in Figure 6. We found excellent fit of the model in equation (2) and $D_{I_0,I_1}(\Delta) < 1$ in all cases for the regions 1, 2, 3, 6 and 7. In the regions 4, 5 and 8, the radii corresponding to the intensity levels 6, 7, and 8 typically had several peaks of $D_{I_0,I_1}(\Delta)$ which exceeded 1 while for the other intensity levels $D_{I_0,I_1}(\Delta)$ was less than one, thus still indicating good overall fit.

Tables 1.1 through 1.8 present the computed μ_{I_0,I_1} and σ_{I_0,I_1}, for all the eight regions, as calculated from the available data. I_0 is shown in the first vertical column, while I_1 increases along horizontal rows starting with the third column. For example, in Table 1.1, 1.796 represents the logarithm of the average distance to I_1 = VI for an earthquake with epicentral intensity I_0 = IX. The corresponding $\sigma_{IX,VI} = 0.101$. The second column in Tables 1.1 through 1.8 shows the total number of earthquakes (isoseismal maps) contributing to the data summarized in that row of tables. For each I_0 and for each μ_{I_0,I_1} and σ_{I_0,I_1} the total number of contributing earthquakes (e.g. 6 for I_0 = IX and I_1 = VI) and the total number of contributing isoseismals (e.g. 73 for I_0 = IX and I_1 = VI) are also presented. From Figure 4 it can be concluded that the number of contributing distances to isoseismals must be less than or equal to 16 times the number of contributing earthquakes.

The values of $\epsilon^{KS}_{I_0,I_1}$ are determined from N_{I_0,I_1} assuming that each isoseismal radius is independent. Since up to 16 radii are contributed by each earthquake, this assumption is violated, and thus $\epsilon^{KS}_{I_0,I_1}$ generally takes a smaller value than what is appropriate. Therefore, even though some of the distributions are rejected by this test, the failure is not regarded as strong evidence that a Gaussian distribution function is inappropriate. For most cases, it is somewhat surprising that a Gaussian distribution function works as well as it does.

ATTENUATION EQUATIONS

For applications, to compute URS or microzonation maps, one needs the probability function $P\{I = I_1|I_0, \Delta\} = P\{I < I_1 + 1|I_0, \Delta\} - P\{I < I_1|I_0, \Delta\}$. For most combinations of I_0 and I_1, this probability can be determined from equation (2) and from Tables 1.1 through 1.8. Unfortunately, for many pairs of I_0 and I_1, the data do not adequately define the statistical parameters and thus there appears to be no alternative other than to find some analytical model which is capable of extrapolating from where data are abundant.

One approach to modeling the mean values, μ_{I_0,I_1} is to use an extension of the method used in Nuttli (1973a,b) and Gupta and Nuttli (1976). One reason for this choice arises from the expected uses in engineering applications and in risk analyses, where log(amplitude) of ground motion is often assumed to be proportional to a numerical value equal to the Roman Numeral which represents a level of MKS intensity. To be consistent with this usage, the model to describe the attenuation of MKS intensity should assume that the intensity is proportional to the log(amplitude) of ground motion. (This assumption is usually not contradicted by the data, Trifunac, 1976; Trifunac and Brady, 1975). Furthermore by making such assumptions, it can be shown that the attenuation of intensity can be described by the attenuation of seismic wave amplitudes.

The equation

$$\left(\frac{A}{T}\right)(D) = K(D)^{-1/2}(\sin D)^{-1/2}e^{-\gamma D} \tag{3}$$

describes the amplitude of the particle velocity in a dispersed surface wave which is not traveling in the Airy phase (Nuttli, 1973b). A is the displacement amplitude of a wave with period T at an epicentral distance D (radians), constant K is related to the amplitude at the source, and γ is the coefficient of inelastic attenuation. For distances greater than

50 km, equation (3) closely approximates the empirical attenuation curve developed by Richter (1958) for the local magnitude scale in Southern California when $\gamma = 0.60/\text{deg}$. Equation (3) also describes the attenuation of $(A/T)_{\max}$ for the vertical component of Rayleigh waves of 3-12 sec period from earthquakes in the central United States when $\gamma = 0.10/\text{deg}$; for the vertical component of 1 sec period *Lg* waves in the same region, and for $\gamma = 0.07/\text{deg}$.

Nuttli (1973a) shows that a selected intensity corresponds to similar values of (A/T) in the eastern and the western United States. This suggests that Modified Mercalli (and MKS) Intensity can be correlated with (A/T), and Gupta and Nuttli (1976) suggest a relationship of the form

$$I_0 - I(D) = a + b \log_{10} \frac{A}{T} \quad . \tag{4}$$

Substituting (3) into (4), approximating $\sin D$ by D, and replacing D with the epicentral distance R (km) leads to

$$I(R) = I_0 + C_1 + C_2(\gamma R \log_{10} e + \log_{10} R) \tag{5}$$

where C_1 and C_2 are new constants. Gupta and Nuttli (1976) used $\gamma = 0.1/\text{deg}$ in equation (5) for the eastern United States, and found $C_1 = 3.7$ and $C_2 = -2.7$ for $R \geq 20$ km.

Equation (5) is a special form of equation (9) in Howell and Schultz (1975). Their paper emphasizes that the preceeding argument is not unique, and that other forms of this attenuation function can be physically motivated. It was shown by Shebalin (1968), for example, that describing the attenuation of seismic energy by use of geometric spreading and inelastic attenuation, leads to the general equation describing the macroseismic field

$$I(\Delta) = bM - \nu_o \log_{10} \Delta - p\Delta + C_o \quad , \tag{6}$$

where M is earthquake magnitude, b, ν_o, p and C_o are constants and $\Delta = (R^2 + H^2)^{1/2}$. M can be approximated by a linear function of the maximum intensity (e.g. $M = 1 +$

$\frac{2}{3}I_0$; Richter, 1958). It is seen that equations (5) and (6) are of equivalent form. If the assumptions involved in the derivation of equation (5) are reasonable, then it should also apply to other parts of the world by using a value of γ appropriate to that region.

For each of the eight chosen regions (Fig. 1) and for the given maximum intensity I_0 the average and the standard deviation of $\log_{10}\Delta = \log_{10}(R^2 + H^2)^{1/2}$ have been computed for each of the intensities I_1 and tabulated in Tables 1.1 through 1.8, when $I_1 = I_0,\ I_0-1,\ I_0-2\ldots$. The average values of $\log_{10}\Delta$ were then fitted by the equations

$$
\begin{aligned}
(1):\ & I_1 - I_0 = b_1 I_0 + b_2 + b_3 \log_{10}\Delta + b_4\Delta/100 \\
(2):\ & I_1 - I_0 = b_2 + b_3 \log_{10}\Delta + b_4\Delta/100 \\
(3):\ & I_1 - I_0 = b_1 I_0 + b_2 + b_3 \log_{10}\Delta + b_4\Delta/100 \\
& \quad + b_5(\Delta/100)I_0 \\
(4):\ & I_1 - I_0 = b_2 + b_3 \log_{10}\Delta + b_4\Delta/100 \\
& \quad + b_5(\Delta/100)I_0 \\
(5):\ & I_1 - I_0 = b_1 I_0 + b_2 + b_3 \log_{10}\Delta + b_4\Delta/100 \\
& \quad + b_5(\Delta/100)I_0 + b_6(\Delta/100)^2 \\
(6):\ & I_1 - I_0 = b_2 + b_3 \log_{10}\Delta + b_4\Delta/100 \\
& \quad + b_5(\Delta/100)I_0 + b_6(\Delta/100)^2 \\
(7):\ & I_1 - I_0 = b_1 I_0 + b_2 + b_3 \log_{10}\Delta + b_4\Delta/100 \\
& \quad + b_5(\Delta/100)I_0 + b_6(\Delta/100)^2 + b_7(\Delta/100)^2 I_0 \\
(8):\ & I_1 - I_0 = b_2 + b_3 \log_{10}\Delta + b_4\Delta/100 \\
& \quad + b_5(\Delta/100)I_0 + b_6(\Delta/100)^2 + b_7(\Delta/100)^2 I_0 \quad .
\end{aligned}
\tag{7}
$$

It is seen that all 8 forms of equation (7) contain the three coefficients: b_2, b_3 and b_4, i.e. that the core of the equations has the same form as equations (5) and (6). Other

coefficients b_1, b_5, b_6 and b_7 and their respective independent values have been indicated by detailed analyses of the attenuation of the averages μ_{I_0,I_1} versus distance Δ.

The results of the regression analysis using equation (7) have been presented in Tables 2.1 through 2.8. For equation (7:4) in Region 1 and under b_3 we find -4.003 and .565. This means that with the 95 percent confidence the value of $b_3 = -4.003 \pm .565$ i.e. this coefficient is significantly different from zero. On the other hand, for example, for equation (7:5) and b_6 we find $-.177$ and .406 i.e. $b_6 = -.177 \pm 0.406$, or this coefficient is not significantly different from zero, and thus could be eliminated from the model equation.

Detailed analysis of the coefficients in Tables 2.1 through 2.8 shows that the best choice for the empirical attenuation equation is the second equation in the above group i.e.

$$I_1 - I_0 = b_2 + b_3 \log_{10} \Delta + b_4 \Delta/100 \quad . \tag{8}$$

Therefore, this equation has been selected for all subsequent analyses in this work. It is equivalent in form to equation (5) if Δ is taken to correspond to R and if $c_1 = b_2$, $c_2 = b_3$ and $\gamma = b_4/(100\ b_3 \log_{10} e)$.

Gupta and Nuttli (1976) used $\gamma = 0.1$/deg (=0.0009/km) for eastern United States while Nuttli (1976) used $\gamma = 0.60$/deg (=0.0054/km) for California. It is interesting to compare these results with the possible interpretation of the results in Tables 2.1 through 2.8. Assuming that some physical analogy can be drawn between equations (3) and (5) or (8) one can compute the values of γ implied by the coefficients b_3 and b_4. These results are summarized in Table 3, and suggest comparable and larger γ than $\gamma = 0.005$/ km in California in regions 1, 2 and 5. In region 6 γ's are comparable and smaller than the estimates for the eastern United States. In regions 3, 4 and 7, γ takes on intermediate values.

Table 2.1 Regression coefficients b_1 through b_7 in equation (7) and their 90 percent confidence intervals.

REGION 1

EQUATION NUMBER	b1	b2	b3	b4	b5	b6	b7
1	6.920 .786	-.375 .052	-3.625 .450	-.202 .280			
2		3.044 .873	-2.641 .664	-.982 .404			
3	6.576 .802	-.290 .075	-3.887 .473	1.197 .955	-.154 .101		
4		4.533 .719	-4.003 .565	3.530 .883	-.441 .081		
5	7.091 1.429	-.310 .089	-4.253 .964	1.495 1.183	-.118 .132	-.177 .406	
6		3.384 1.115	-2.856 1.023	2.128 1.363	-.493 .089	.544 .407	
7	6.849 1.444	-.203 .133	-4.850 1.111	5.415 3.847	-.494 .376	-2.206 1.937	.216 .202
8		5.519 1.175	-5.084 1.125	9.781 2.635	-1.005 .176	-4.161 1.488	.446 .137

Table 2.2

REGION 2

EQUATION NUMBER	b1	b2	b3	b4	b5	b6	b7
1	.998 1.108	.312 .130	-3.548 .408	.043 .071			
2		1.662 1.111	-2.247 .676	-.045 .119			
3	1.439 1.427	.214 .235	-3.239 .742	-1.254 2.587	.126 .251		
4		2.572 .691	-2.727 .482	-3.192 1.458	.315 .141		
5	2.139 1.403	.311 .229	-4.488 .963	.999 2.726	-.036 .253	-.038 .020	
6		3.592 .922	-3.583 .707	-2.037 1.585	.251 .142	-.032 .020	
7	1.282 1.685	.474 .290	-4.985 1.102	5.526 5.668	-.472 .542	-2.141 2.321	.209 .231
8		3.601 .946	-3.581 .723	-2.335 3.110	.280 .297	.181 1.905	-.021 .190

Table 2.3 Regression coefficients b_1 through b_7 in equation (7) and their 90 percent confidence intervals.

REGION 3

EQUATION NUMBER	b1	b2	b3	b4	b5	b6	b7
1	4.009 .714	-.043 .058	-3.547 .443	-.371 .295			
2		3.547 .523	-3.431 .414	-.476 .276			
3	3.438 .732	.100 .087	-4.071 .488	2.466 1.356	-.285 .133		
4		3.985 .559	-3.852 .451	1.316 .921	-.167 .086		
5	3.301 1.117	.102 .089	-3.943 .924	2.304 1.695	-.291 .140	.065 .397	
6		3.973 .955	-3.838 .923	1.298 1.457	-.168 .090	.007 .395	
7	2.959 1.134	.226 .128	-4.626 1.047	7.070 3.947	-.736 .361	-2.292 1.810	.240 .180
8		3.990 1.002	-3.858 .982	1.422 2.385	-.178 .180	-.079 1.346	.008 .127

Table 2.4

REGION 4

EQUATION NUMBER	b1	b2	b3	b4	b5	b6	b7
1	7.258 .969	-.218 .061	-4.428 .507	-.008 .227			
2		4.397 .714	-3.682 .495	-.371 .220			
3	7.368 .980	-.285 .098	-4.091 .640	-.954 1.113	.088 .102		
4		5.891 .915	-4.728 .657	1.347 .853	-.141 .070		
5	7.694 1.653	-.293 .105	-4.315 1.116	-.805 1.279	.099 .111	-.049 .197	
6		5.170 1.507	-4.114 1.212	.804 1.243	-.151 .072	.123 .204	
7	7.895 1.608	-.129 .136	-5.699 1.328	4.773 3.342	-.369 .282	-2.397 1.320	.225 .125
8		7.346 1.497	-6.137 1.243	7.134 2.230	-.595 .150	-3.181 1.027	.305 .093

Table 2.5 Regression coefficients b_1 through b_7 in equation (7) and their 90 percent confidence intervals.

REGION 5

EQUATION NUMBER	b1	b2	b3	b4	b5	b6	b7
1	2.113 1.101	-.030 .094	-2.054 .673	-.742 .322			
2		1.936 .914	-2.102 .652	-.732 .315			
3	1.446 1.244	.108 .154	-2.382 .730	.805 1.399	-.163 .144		
4		2.020 .936	-2.184 .670	.053 .901	-.083 .087		
5	.175 1.563	.121 .153	-1.248 1.122	-.556 1.726	-.172 .143	.297 .225	
6		.865 1.295	-1.071 1.095	-1.342 1.410	-.082 .087	.286 .223	
7	.915 1.896	-.050 .289	-.700 1.374	-4.396 5.755	.223 .582	1.623 1.909	-.144 .205
8		.681 1.305	-.835 1.116	-3.503 2.486	.130 .219	1.348 1.031	-.114 .108

Table 2.6

REGION 6

EQUATION NUMBER	b1	b2	b3	b4	b5	b6	b7
1	9.966 3.907	.097 .070	-5.266 2.081	-.171 .417			
2		10.498 3.966	-5.246 2.120	-.130 .424			
3	10.669 4.010	.246 .185	-6.212 2.357	.597 .977	-.079 .091		
4		9.855 4.029	-4.861 2.163	-.474 .563	.033 .035		
5	5.451 12.913	.248 .188	-3.001 7.910	-.778 3.376	-.082 .093	.150 .351	
6		5.105 13.151	-1.931 8.015	-1.732 3.359	.032 .036	.136 .357	
7	5.926 13.642	.313 .495	-3.558 8.973	-.124 5.710	-.143 .442	.040 .845	.012 .086
8		4.019 13.108	-1.139 7.998	-2.950 3.505	.130 .093	.483 .467	-.038 .033

Table 2.7 Regression coefficients b_1 through b_7 in equation (7) and their 90 percent confidence intervals.

REGION 7

EQUATION NUMBER	b1	b2	b3	b4	b5	b6	b7
1	5.731 1.217	-.147 .075	-3.260 .613	-.326 .188			
2		4.694 1.050	-3.411 .650	-.268 .187			
3	5.638 1.304	-.123 .125	-3.339 .706	-.129 .826	-.019 .078		
4		4.890 1.056	-3.542 .675	.468 .556	-.079 .048		
5	3.912 2.218	-.088 .131	-2.245 1.339	-.625 .974	-.052 .085	.104 .108	
6		3.084 1.816	-2.165 1.314	-.328 .855	-.098 .049	.125 .102	
7	4.216 2.139	.114 .179	-3.858 1.640	4.007 3.066	-.432 .254	-1.136 .789	.117 .074
8		4.660 1.989	-3.446 1.482	2.488 1.904	-.294 .129	-.794 .569	.083 .051

Table 2.8

REGION 8

EQUATION NUMBER	b1	b2	b3	b4	b5	b6	b7
1	6.563 1.596	-.032 .107	-4.499 .958	.360 .412			
2		6.360 1.383	-4.532 .927	.372 .400			
3	4.982 1.843	.173 .169	-4.477 .915	2.040 1.168	-.220 .144		
4		6.249 1.369	-4.458 .917	1.145 .776	-.103 .087		
5	-1.299 2.164	.079 .123	1.399 1.734	-5.103 2.123	-.067 .111	1.210 .331	
6		-.972 2.055	1.621 1.660	-5.755 1.821	-.010 .065	1.254 .316	
7	-.622 2.591	-.003 .204	1.343 1.792	-6.463 3.437	.123 .388	1.719 1.048	-.070 .137
8		-.643 2.114	1.341 1.711	-6.422 2.004	.118 .166	1.707 .625	-.069 .081

Table 3 Coefficient of "anelastic attenuation γ" for different regions computed from $\gamma = b_4/(100 b_3 \log_{10} e)$.

	b_3	γ
1	-2.64 +/- 0.66	0.0087
2	-2.27 +/- 2.18	0.0081
3	-3.43 +/- 0.41	0.0032
4	-3.68 +/- 0.50	0.0023
5	-2.10 +/- 0.65	0.0080
6	-5.25 +/- 2.12	0.00057
7	-3.41 +/- 0.65	0.0018
8	-4.53 +/- 0.93	------

With larger data base and with more detailed analyses of the validity of such inferences, it may become possible to associate the above variations in γ with the details of the tectonic regime in the Balkan region. Having better established the underlying physical similarities of this area relative to the western United States, it may also become possible to use such inferences to justify the use of the data recorded in the western United States, for engineering design in appropriate regions of the Balkan countries and vice versa.

Tables 4.1 through 4.8 present averages and standard deviations of the logarithm of the hypocentral distance to the isoseism enclosing $I \geq I_1$. These tables have been computed by using equation (8) and represent smooth surfaces through an available data represented by the Tables 1.1 through 1.8.

In Figure 7, different attenuation equations, for eight regions, have been plotted on the same scale for $I_0 = \text{X}$ and versus distance $\Delta = (R^2 + H^2)^{1/2}$. For comparison, the average attenuation equations applicable to the western and central and eastern United States (assuming $H = 0$) have been plotted also. Except for Regions 6 and 7 it is seen that the overall slope of all other attenuation equations is very similar to that in the western United States. Translation of these curves, relative to each other and relative to the western United States data can be explained by the variation of the average focal depth of earthquakes in the respective regions. Region 3, for example, which has the "lowest" attenuation curve in Figure 6, has many shallow sources, many less than 10 km, and most less than 20 km deep (Figure 5c). Region 7 which has the "largest" attenuation curve amplitudes in this group has deeper earthquakes, between 10 and 60 km. The attenuation equation for Region 8 (south-western Turkey) is similar to the equation for the central and eastern United States (Trifunac et al., 1979).

Table 4.1 Computed average and standard deviation of the logarithm of the hypocentral distance in kilometers to isoseism enclosing the area with $I \geq I_1$.

REGION 1

EPICENTRAL INTENSITY, I_o	3	4	5	6	7	8	9	10
3.0	1.105 .154							
4.0	1.431 .160	1.105 .154						
5.0	1.716 .188	1.431 .160	1.105 .154					
6.0	1.954 .151	1.716 .188	1.431 .160	1.105 .154				
7.0	2.146 .149	1.954 .151	1.716 .188	1.431 .160	1.105 .154			
8.0	2.302 .145	2.146 .149	1.954 .151	1.716 .188	1.431 .160	1.105 .154		
9.0	2.428 .082	2.302 .145	2.146 .149	1.954 .151	1.716 .188	1.431 .160	1.105 .154	
10.0	2.533 .162	2.428 .082	2.302 .145	2.146 .149	1.954 .151	1.716 .188	1.431 .160	1.105 .154

Table 4.2

REGION 2

EPICENTRAL INTENSITY, I_o	3	4	5	6	7	8	9	10
3.0	.739 .159							
4.0	1.182 .166	.739 .159						
5.0	1.622 .192	1.182 .166	.739 .159					
6.0	2.052 .192	1.622 .192	1.182 .166	.739 .159				
7.0	2.462 .156	2.052 .192	1.622 .192	1.182 .166	.739 .159			
8.0	2.829 .058	2.462 .156	2.052 .192	1.622 .192	1.182 .166	.739 .159		
9.0	3.135 .172	2.829 .058	2.462 .156	2.052 .192	1.622 .192	1.182 .166	.739 .159	
10.0	3.376 .172	3.135 .172	2.829 .058	2.462 .156	2.052 .192	1.622 .192	1.182 .166	.739 .159

INTENSITY, I_1

Table 4.3 Computed average and standard deviation of the logarithm of the hypocentral distance in kilometers to isoseism enclosing the area with $I \geq I_1$.

REGION 3

EPICENTRAL INTENSITY, I_o	INTENSITY, I_1							
	3	4	5	6	7	8	9	10
3.0	1.019 .182							
4.0	1.298 .201	1.019 .182						
5.0	1.566 .209	1.298 .201	1.019 .182					
6.0	1.817 .231	1.566 .209	1.298 .201	1.019 .182				
7.0	2.045 .198	1.817 .231	1.566 .209	1.298 .201	1.019 .182			
8.0	2.246 .117	2.045 .198	1.817 .231	1.566 .209	1.298 .201	1.019 .182		
9.0	2.418 .036	2.246 .117	2.045 .198	1.817 .231	1.566 .209	1.298 .201	1.019 .182	
10.0	2.564 .201	2.418 .036	2.246 .117	2.045 .198	1.817 .231	1.566 .209	1.298 .201	1.019 .182

Table 4.4

REGION 4

EPICENTRAL INTENSITY, I_o	INTENSITY, I_1							
	3	4	5	6	7	8	9	10
3.0	1.179 .142							
4.0	1.438 .165	1.179 .142						
5.0	1.688 .172	1.438 .165	1.179 .142					
6.0	1.924 .196	1.688 .172	1.438 .165	1.179 .142				
7.0	2.141 .185	1.924 .196	1.688 .172	1.438 .165	1.179 .142			
8.0	2.334 .142	2.141 .185	1.924 .196	1.688 .172	1.438 .165	1.179 .142		
9.0	2.503 .117	2.334 .142	2.141 .185	1.924 .196	1.688 .172	1.438 .165	1.179 .142	
10.0	2.647 .169	2.503 .117	2.334 .142	2.141 .185	1.924 .196	1.688 .172	1.438 .165	1.179 .142

Table 4.5 Computed average and standard deviation of the logarithm of the hypocentral distance in kilometers to isoseism enclosing the area with $I \geq I_1$.

REGION 5

EPICENTRAL INTENSITY, I_o	INTENSITY, I_1							
	3	4	5	6	7	8	9	10
3.0	.894 .206							
4.0	1.324 .212	.894 .206						
5.0	1.699 .186	1.324 .212	.894 .206					
6.0	2.000 .208	1.699 .186	1.324 .212	.894 .206				
7.0	2.231 .179	2.000 .208	1.699 .186	1.324 .212	.894 .206			
8.0	2.408 .126	2.231 .179	2.000 .208	1.699 .186	1.324 .212	.894 .206		
9.0	2.547 .201	2.408 .126	2.231 .179	2.000 .208	1.699 .186	1.324 .212	.894 .206	
10.0	2.660 .201	2.547 .201	2.408 .126	2.231 .179	2.000 .208	1.699 .186	1.324 .212	.894 .206

Table 4.6

REGION 6

EPICENTRAL INTENSITY, I_o	INTENSITY, I_1							
	3	4	5	6	7	8	9	10
3.0	1.978 .192							
4.0	2.156 .152	1.978 .192						
5.0	2.330 .117	2.156 .152	1.978 .192					
6.0	2.496 .114	2.330 .117	2.156 .152	1.978 .192				
7.0	2.653 .121	2.496 .114	2.330 .117	2.156 .152	1.978 .192			
8.0	2.799 .154	2.653 .121	2.496 .114	2.330 .117	2.156 .152	1.978 .192		
9.0	2.933 .154	2.799 .154	2.653 .121	2.496 .114	2.330 .117	2.156 .152	1.978 .192	
10.0	3.055 .154	2.933 .154	2.799 .154	2.653 .121	2.496 .114	2.330 .117	2.156 .152	1.978 .192

Table 4.7 Computed average and standard deviation of the logarithm of the hypocentral distance in kilometers to isoseism enclosing the area with $I \geq I_1$.

REGION 7

EPICENTRAL INTENSITY, I_o	INTENSITY, I_1							
	3	4	5	6	7	8	9	10
3.0	1.358 .202							
4.0	1.635 .197	1.358 .202						
5.0	1.900 .152	1.635 .197	1.358 .202					
6.0	2.146 .106	1.900 .152	1.635 .197	1.358 .202				
7.0	2.366 .064	2.146 .106	1.900 .152	1.635 .197	1.358 .202			
8.0	2.558 .072	2.366 .064	2.146 .106	1.900 .152	1.635 .197	1.358 .202		
9.0	2.721 .052	2.558 .072	2.366 .064	2.146 .106	1.900 .152	1.635 .197	1.358 .202	
10.0	2.860 .154	2.721 .052	2.558 .072	2.366 .064	2.146 .106	1.900 .152	1.635 .197	1.358 .202

Table 4.8

REGION 8

EPICENTRAL INTENSITY, I_o	INTENSITY, I_1							
	3	4	5	6	7	8	9	10
3.0	1.425 .158							
4.0	1.662 .098	1.425 .158						
5.0	1.911 .066	1.662 .098	1.425 .158					
6.0	2.193 .044	1.911 .066	1.662 .098	1.425 .158				
7.0	2.666 .057	2.193 .044	1.911 .066	1.662 .098	1.425 .158			
8.0	2.725 .100	2.453 .057	2.181 .044	1.911 .066	1.662 .098	1.425 .158		
9.0	2.997 .100	2.725 .100	2.453 .057	2.181 .044	1.911 .066	1.662 .098	1.425 .158	
10.0	3.270 .100	2.997 .100	2.725 .100	2.453 .057	2.181 .044	1.911 .066	1.662 .098	1.425 .158

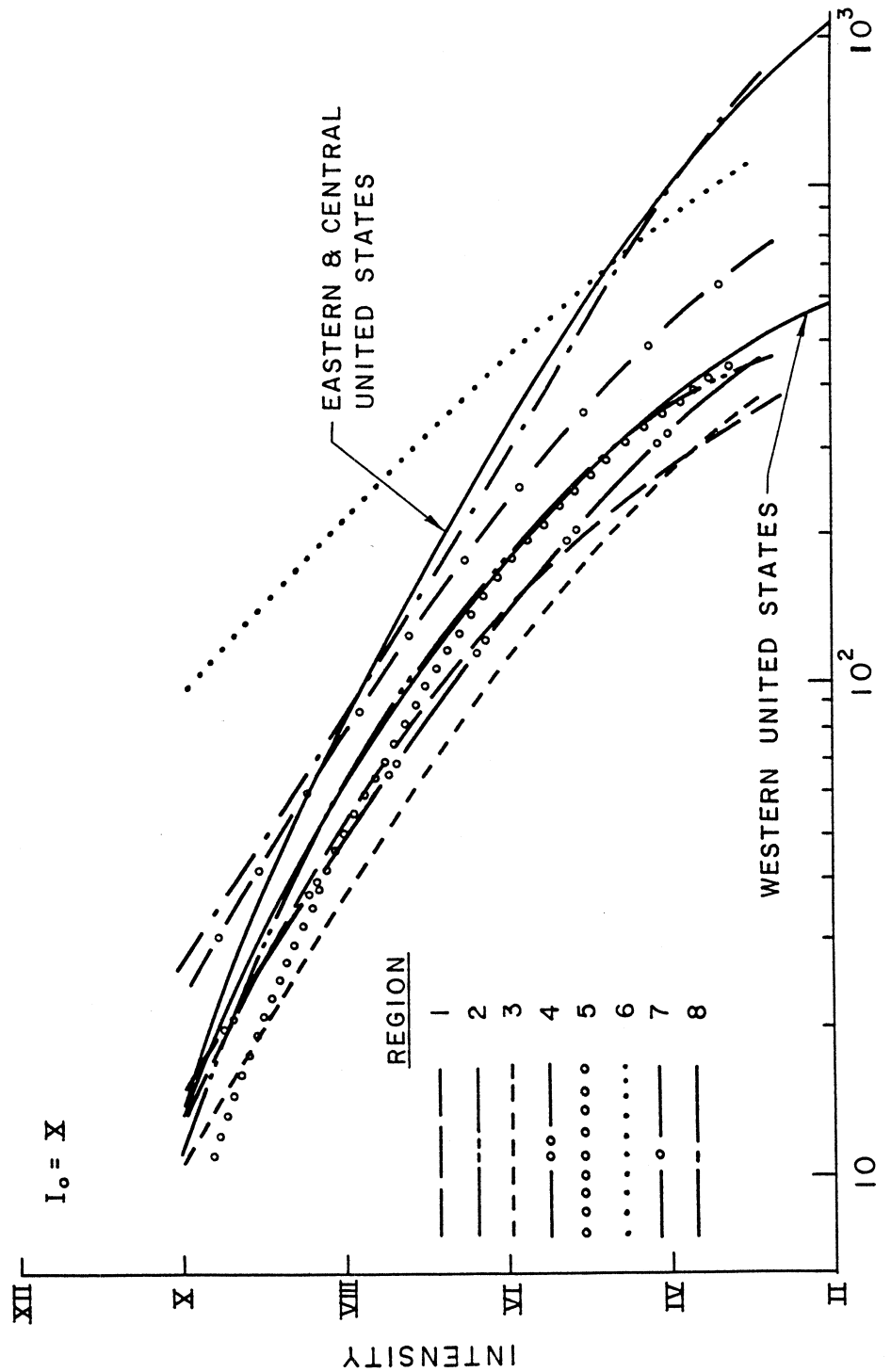

Figure 7 Comparison of the attenuation of MKS intensities with hypocentral distance in regions 1, 2,..., 7 and 8, for $I_0 = X$, with attenuation of MMI in the western and eastern United States (for $\Delta = R$ i.e. when H is not considered explicitly.

DISCUSSION AND CONCLUSIONS

The quality and reliability of the estimates for the mean and for the standard deviations of the distances for a given isoseismal depend on the number of radii used in the analysis. Trifunac et al. (1979) and Gupta and Trifunac (1988) found that about 100 radii, or contributions from at least 7 earthquakes are needed, assuming that each earthquake contributes up to 16 radii. Consequently, from μ_{I_0,I_1} and σ_{I_0,I_1} which are determined by 100 or more radii to isoseism boundaries can be considered "well-determined." Perusal of Tables 1.1 through 1.8 will give the reader detailed impression on how reliable and how many good estimates there are in the data, region by region.

For intensities III and smaller, the average radii to isoseism tend to increase more slowly, relative to the radii for intensities IV, than one would expect from the corresponding increases at the higher levels of intensity. Such trends were observed also in previous studies (e.g. Everenden et al., 1973; Trifunac et al., 1979; Gupta and Trifunac, 1988) and suggest that these small intensities are at the threshold level of human perception, about 5-10 cm/sec^2 ground acceleration for intensity III (Trifunac and Brady, 1975). Several average radii, $\mu(I_0, I_1)$ in Tables 1.1 through 1.8 fall in this category and thus should be considered suspect and not representative of this data base. Some obvious examples of these for $I_1 =$ III are $\mu = 2.149$ for $I_0 =$ VII-VIII (i.e. 7.5) in Table 1.1, and $\mu = 2.141$ for $I_0 =$ VIII in Table 1.5, but other less obvious cases are undoubtedly present in the data base for $I_1 =$ III.

Some uncertainties and scatter in the data occur because the epicentral intensity may not be determined with sufficient accuracy and because the discrete levels of the intensity scale, through discretization of the continuous physical process inevitably increase the scatter of the overall data on the radii to I_1. The maps of all earthquakes considered in this study (Shebalin et al., 1974) have I_0 identified either by a discrete level, say X, or

by the range e.g. IX to X. To improve the situation somewhat, we have assigned numerical values corresponding to the Roman numerals of the MKS scale, $I_0 = 9.5$ to an earthquake labeled by I_0 = IX to X, for example. This reduces the discretization error slightly, but does not elliminate it. This, of course, assumes that the levels of the discrete descriptive scale can be assigned to the uniformly increasing numerical scale. Past analyses have shown that this convenient but not physical assumption is not seriously violated by the observed data and by other available inferences on the intensity scales (Trifunac, 1976; Trifunac and Brady, 1975; Trifunac, 1978; 1979). Assumption of this type could be avoided by the use of indicator variables, but that would require considerably larger data base than what is available at present.

Another problem with estimation of intensities near epicenter is that there is usually only a small number of independent estimates on the effects of shaking just above the earthquake. On the other hand, smaller intensities away from epicenter cover larger areas, thus producing many more sampling points, and the contouring process tends to average out the uncertainties there. Thus, the quality and the reliability of μ_{I_0,I_1} and σ_{I_0,I_1} are low at or near I_0, then improve for intermediate distances, and again become worse as I_1 approaches the threshold level of perseptibility, at larger distances.

Previous studies by Anderson (1978) and Gupta and Trifunac (1988) used epicentral distance to analyze the distribution functions of the radii to isoseismals although it has been suggested that regional differences in the average depth of earthquakes (Howell and Schultz, 1975), would suffice to exaplin the differences in the average attenuation rates for different geologic provinces. Thus, when the data on focal depths is available, inclusion of this information into the regression analyses of the distribution of the radii should reduce the scatter and the uncertainties in the results. We chose to take advantage of this approach in this investigation, by carrying out all the analyses described here in terms of $\Delta = (R^2 + H^2)^{1/2}$ rather than R alone as in Anderson (1978) and Gupta and Trifunac

(1988). We chose this approach aware of the fact that many focal depths for the data in the final report on the Balkan Project (Shebalin et al., 1974) have been determined in terms of the macroseismic data for the same earthquakes, and not by some other independent means.

Another factor which also influences the rate of attenuation of intensities with distance, and which interacts with the effects of the focal depth, is the size of the fault surface. This effect is particularly significant for shallow earthquakes and for the shape of attenuation with respect to R (or Δ) for the distribution of radii of I_0 and I_1 near I_0. The finite dimensions of the sources and its effects on the inferences about this data base were neither considered in the Balkan project (Shebalin, 1974), nor in this study.

As in Anderson (1978), the radii, R_i, in this work were measured from the geometrical center of the isoseismal bounding the area assigned to I_0. In all instances the epicentral coordinates have been identified in this manner and not from some other independent or instrumental determination. Using the instrumentally determined epicenters, if those were available, would have increased the variation of the measured radii, because it is possible that for many (relatively larger) earthquakes the "epicenter" of I_0 isoseismal does not coinside with the instrumentally determined epicenter.

Figure 7 suggests that, except for Region 6 which is quite different (deep earthquakes) and Region 8, which resembles the attenuation of mean intensities in the eastern United States, the attenuation in all other areas of Balkan seem to be very similar to the attenuation of mean intensities in the western United States. Large standard deviations of all estimates in Tables 1.1 through 1.8 suggest that the method of analysis in this paper is not well suited to study the details of the differences in attenuation and to detect small differences which are clearly overshadowed by the large scatter in the data. In any case for the same average depth of foci one would not expect to see significant differences in

the shapes of the average attenuation curves for $\Delta < 100$ to 200 km, even if the respective geological environments were quite different. The distance range $0 < \Delta < 200$ km is of particular interest to earthquake engineering, because the damaging motions typically occur there, and because the calculations show that the contributions to seismic risk estimates are very significant within this distance range (Westermo et al., 1980). Therefore, Figure 7 also suggests that the assumption that the attenuation in most regions (except regions 6 and 8) of the Balkan is similar to that in California (and the western United States) is not contradicted by the data which is considered in this work. This suggests that some other related characteristics of strong ground motion, for example, relationship between the discrete levels of the intensity of shaking and of the characteristics of recorded strong ground motion might be similar as well. Such assumptions must be carefully verified, before detailed seismic risk calculations can be carried out in the Balkan region, using computer programs developed and "calibrated" for the western United States. An indication that the physical characteristics of the two respective environments are not too dissimilar suggests better and simpler ways for careful calibration and translation of the experiences from one region with abundant data to another where the data is not adequate at present to arrive at independent estimates.

REFERENCES

Anderson, J. G. and M. D. Trifunac (1977). Uniform Risk Functionals for Characterization of Strong Earthquake Ground Motion, Dept. of Civil. Eng. Rep. No. 77-02, Univ. Southern California, Los Angeles, California.

Anderson, J. G. (1978). On Attenuation of Modified Mercalli Intensity with Distance in the United States, Bull. Seism. Soc. Amer., Vol. 68, 1147-1179.

Bollinger, G. A. (1977). Reinterpretation of the Intensity Effects of the 1886 Charleston, South Carolina, Earthquake, in Geological Geophysical and Seismological Studies related to Charleston, South Carolina Earthquake of 1886; a preliminary report, D. W. Rankin, editor, U. S. Geological Survey Profess. Paper 1028.

Everenden, J. F., R. R. Hibbard and J. S. Schneider (1973). Interpretation of Seismic Intensity Data, Bull. Seism. Soc. Amer., *63,* 399-422.

Gupta, I. N. and O. W. Nuttli (1976). Spatial Attenuation of Intensities for Central U.S. Earthquakes, Bull. Seism. Soc. Amer., *66,* 743-751.

Gupta, I. D. and M. D. Trifunac (1988). Attenuation of Intensity with Epicentral Distance in India, Int. J. Soil Dynamics and Earthquake Eng. (in press).

Hoel, P. G. (1971). Introduction to Mathematical Statistics, J. Wiley and Sons, New York.

Howell, B. F. and T. R. Schultz (1975). Attenuation of Modified Mercalli Intensity with Distance from the Epicenter, Bull. Seism. Soc. Amer., *65,* 651-665.

Jordanovski, L., V. W. Lee, M. Manić, T. Olumčeva, C. Sinadinovski, M. Todorovska and M. D. Trifunac (1987). Strong Earthquake Ground Motion Data in EQINFOS: YUGOSLAVIA, Part I, Dept. Civil Eng. Rep. No. 87-05, Univ. Southern California, Los Angeles, California.

Lee, V. W. and M. D. Trifunac (1985). Uniform Risk Spectra of Strong Earthquake Ground Motion, Dept. Civil Eng. Rep. No. 85-05, Univ. Southern California, Los Angeles, California.

Lee, V. W. (1987). Seismic Microzonation Method Based on Modified Mercalli Intensity Scaling, Earthquake Eng. and Engineering Vibration, Vol. 7, No. 3, 47-63.

Lee, V. W. and M. D. Trifunac (1987). Microzonation of a Metropolitan Area, Dept. of Civil Eng. Rep. No. 87-02, Univ. Southern California, Los Angeles, California.

Nuttli, O. W. (1973a). The Mississippi Valley Earthquakes of 1811 and 1812: Intensities, Ground Motions and Magnitudes, Bull. Seism. Soc. Amer., *63,* 227-248.

Nuttli, O. W. (1973b). Seismic Wave Attenuation and Magnitude Relations for Eastern North America, J. Geophys. Res., *78,* 876-885.

Nuttli, O. W. (1976). Comments on "Seismic Intensities, 'Size' of Earthquakes and Related Parameters," by Jack F. Everenden, Bull. Seism. Soc. Amer., *66,* 331-338.

Richter, C. F. (1958). Elementary Seismology, Freeman and Co. San Francisco.

Shebalin, N. V. (1968). Metody ispolzovaniya inzhenerno- seismologicheskikh dannykh pri seismicheskom rayonirovanni, Seismicheskoye rayonirovaniye SSSR, Nauka, 1968.

Shebalin, N. V. (1969). Makroseismicheskoye pole i ochag silnogo zemletryaseniya, Dissertation, Institute of the Physics of the Earth, Moscow.

Shebalin, N. V., V. Kárnik and O. Hadžievski (editors) (1974). Catalogue of Earthquakes (Part I, 1901-1970, Part II, prior to 1901). UNDP/UNESCO Survey of the Seismicity of the Balkan Region, UNESCO, Skopje, Yugoslavia.

Trifunac, M. D. and A. G. Brady (1975). On the Correlation of Seismic Intensity Scales with the Peaks of Recorded Strong Ground Motion, Bull. Seism. Soc. Amer., *65,* 139-162.

Trifunac, M. D. (1976). A Note on the Range of Peak Amplitudes of Recorded Accelerations, Velocities and Displacements with Respect to the Modified Mercalli Intensity, Earthquake Notes Vol. 47, No. 2, 9-24.

Trifunac, M. D. (1978). Response Spectra of Earthquake Ground Motion, ASCE, EM5, Vol. 104, 1081-1097.

Trifunac, M. D. (1979). Preliminary Empirical Model for Scaling Fourier Amplitude Spectra of Strong Motion Accelertion in Terms of Modified Mercalli Intensity and Geologic Site Conditions, Int. J. Earthquake Eng. and Struct. Dynamics, 1, 63-74.

Trifunac, M. D., J. G. Anderson, B. D. Westermo, H. L. Wong (1979). Methods for Prediction of Strong Earthquake Ground Motion, U.S. Nuclear Regulatory Commission, NUREG/CR-0689, Washington, D.C.

Trifunac, M. D. and V. W. Lee (1987a). Empirical Models for Scaling Fourier Amplitude Spectra of Strong Motion Acceleration in Terms of Earthquake Magnitude, Source to Station Distance, Site Intensity and Recording Site Conditions, Int. J. Soil Dynamics and Earthquake Eng. (in press).

Trifunac, M. D. and V. W. Lee (1987b). Empirical Models for Scaling Pseudo Relative Velocity Spectra of Strong Earthquake Accelerations, in Terms of Magnitude, Distance, Site Intensity and Recording Site Conditions, Int. J. Soil Dynamics and Earthquake Eng. (in press).

Trifunac, M. D. and V. W. Lee (1987c). Direct Empirical Scaling of Response Spectral Amplitudes for Various Site and Earthquake Parameters, U.S. Nuclear Regulatory Commission, Report NUREG/CR-4903, Vol. 1.

Trifunac, M. D., J. G. Anderson and V. W. Lee (1987d). Methods for Introduction of Geological Data Into Characterization of Active Faults and Seismicity and Upgrading of the Uniform Risk Spectrum Technique, U.S. Nuclear Regulatory Commission, Report NUREG/CR-4903, Vol. 2.

Trifunac, M. D. (1988). A Microzonation Method Based on Uniform Rick Spectra, Int. J. Soil Dynamics and Earthquake Eng. (in press).

Westermo, B. D., M. D. Trifunac, J. G. Anderson and M. Dravinski (1980). Seismic Risk Tables for Pseudo Relative Velocity Spectra in Regions with Shallow Seismicity, Dept. Civil Eng. Rep. No. 80-01, Univ. Southern California, Los Angeles, California.